ENTANGLEMENT GENERATION AND APPLICATIONS IN QUANTUM INFORMATION

A Dissertation

by

TIEGANG DI

Submitted to the Office of Graduate Studies of
Texas A&M University
in partial fulfillment of the requirements for the degree of

DOCTOR OF PHILOSOPHY

May 2006

Major Subject: Physics

ENTANGLEMENT GENERATION AND APPLICATIONS IN QUANTUM INFORMATION

A Dissertation

by

TIEGANG DI

Submitted to the Office of Graduate Studies of
Texas A&M University
in partial fulfillment of the requirements for the degree of

DOCTOR OF PHILOSOPHY

Approved by:

Chair of Committee,	M. Suhail Zubairy
Committee Members,	Marlan Scully
	Olga Kocharovskaya
	Philip Hemmer
Head of Department,	Edward S. Fry

May 2006

Major Subject: Physics

ABSTRACT

Entanglement Generation and Applications
in Quantum Information. (May 2006)
Tiegang Di, B.S.; M.S., JiLin University;
M.S., Texas A&M University
Chair of Advisory Committee: M. Suhail Zubairy

This dissertation consists of three sections. In the first section, we discuss the generation of arbitrary two-qubit entangled states and present three generation methods. The first method is based on the interaction of an atom with classical and quantized cavity fields. The second method is based on the interaction of two coupled two-level atoms with a laser field. In the last method, we use two spin-1/2 systems which interact with a tuned radio frequency pulse. Using those methods we have generated two qubit arbitrary entangled states which is widely used in quantum computing and quantum information. In the second section, we discuss a possible experimental implementation of quantum walk which is based on the passage of an atom through a high-Q cavity. The chirality is determined by the atomic states and the displacement is characterized by the photon number inside the cavity. Our scheme makes quantum walk possible in a cavity QED system and the results could be widely used on quantum computer. In the last section, we investigate the properties of teleporting an arbitrary superposition of entangled Dicke states of any number of atoms (qubits) between two distant cavities. We also studied teleporting continuous variables of an optical field. Teleportation of Dicke states relies on adiabatic passage using multi-atom dark states in each cavity and a conditional detection of photons leaking out

of both cavities. In the continuous variables teleportation scheme we first reformulate the protocol of quantum teleportation of arbitrary input optical field states in the density matrix form, and established the relation between the P-function of the input and output states. We then present a condition involving squeeze parameter and detection efficiency under which the P-function of the output state becomes the Q function of the input state such that any nonclassical features in the input state will be eliminated in the teleported state. Based on the research in this section we have made it possible of arbitrary atomic Dicke states teleportation from one cavity to another, and this teleortation will play an essential role in quantum communication. Since quantum properties is so important in quantum communication, the condition we give in this section to distinguish classical and quantum teleportation is also important.

To My Wife Li Li, My Daughter Catherine and My Family

ACKNOWLEDGMENTS

I would like to express my appreciation to all the people who gave me support in my quantum optical research during the past four years. First and foremost, I want to thank my advisor, Professor M. Suhail Zubairy, without whom I could not have made so much progress in so short a time. I have been privileged to benefit from his deep and wide knowledge in many fields of physics, especially in quantum optics and quantum information. I would like to thank him for supporting me for all these years. My heart was warmed when he showed so much kindness to me, especially when I encountered difficulties in my life. I would like to thank him for so many years' personal care to me, to my family. I experienced a very happy time during my Ph.D studying with him. Next I want to give my thanks to Professor Cheming Ko who was my advisor when I studied in the high energy group, It is he who enabled me to enter TAMU and to begin my microworld research in such a famous university. I will always be very grateful for his guidance and friendship. I especially want to give my thanks to Professor Marlan Scully, who taught me a lot of quantum optical knowledge and helped me to get a better understanding of it. I would like to thank him for all the kindness he has shown me.

I would like to thank Professors Mark Hillery, Shiyao Zhu, Fuli Li, Yaping Yang, Dr. Joerg Evers, and Dr. Ashok Muthukrishnan. During my collaboration with them I learned a lot and I am lucky to have worked with them. I would like to acknowledge and thank all my teachers and professors in the Department of Physics at TAMU and I want very much to give my thanks to my friends: Noam Erez, Han Xiong, Juntao Chang and Qingqing Sun. Their friendship has given me the power of purchasing a Ph.D. I am very happy to study with them.

TABLE OF CONTENTS

LIST OF FIGURES

FIGURE Page

CHAPTER I

INTRODUCTION

Quantum entanglement constitutes perhaps the single most characteristic property that makes quantum mechanics distinct from any classical theory. Entangled states are employed not only to test the foundations of quantum mechanics such as in Bell's inequalities, but they also play a central role in various quantum information processes ranging from quantum teleportation, quantum dense coding and quantum cryptography to quantum computing. So it is obvious that quantum entanglement lies at the heart of quantum computing and quantum informatics. The question of how to generate quantum entangled states has attracted much attention.

Quantum entanglement, which is associated with peculiar nonclassical correlations was first introduced by Einstein, Podolsky, and Rosen(EPR) [1]. Later they turned out to be essential to performing quantum computational and quantum information tasks that are impossible for classical systems [2, 3, 4, 5]. Quantum entangled states consist of finite dimensional states and continuous variable states [6] in Hilbert space. Most of those implementations use atomic states, photonic states or spin states as basis. Many methods of the quantum state engineering inside a cavity have been proposed in the literature. These include methods based on atom-field entanglement [7, 8, 9] and quantum state mapping between multilevel atoms and cavity fields[10]. Several schemes have been proposed to create paticular entangled states. Some papers introduced ways to generate particular entangled states using cavity QED methods. These include Bell basis state [11], the GHZ state [12], states with fixed total photon numbers [13]. Generation of two cavities entangled state of fixed number of photons

---

This dissertation follows the style of *Physical Review A*.

and generation entanglement by passive optical devices has been studied [14, 15]. A generation of arbitrary superposition of Dicke states has been proposed recently [16] using trapped ions [17] whose energy levels represent basis vectors for a qubit. Trapped-ion techniques make it possible to study interactions between photons and a few trapped ions inside a cavity. Kimble et al. produced arbitrary superpositions of Dicke states based on this technique, and showed how to generate arbitrary two photon states [18].

Without a cavity, using atom-field interactions it is also possible to make entangled states. It is well known that the generation of a one-qubit arbitrary atomic state can be realized by using the interaction of an atom with a classical field in a two-level atomic system[19]. For the two qubit case, properties of multi-atom systems have used to generate entangled atomic or photonic states [20, 21], and to create two-atom system entanglement such as pairwise atomic states [22, 23]. Recent studies of multi-atom systems made special entangled states available via the control of the quantum phase [24].

The investigation of spin entanglements has had a long history since EPR paradox was first introduced, for example the spin entanglement was studied when Bennett et al. [25] proposed the first protocol for quantum teleportion. Compared with atomic states or photonic states, spin states are more stable. In contrast atomic-photon system will collapse soon due to decoherence. This is a important advantage in quantum computing and quantum information. Recently, some schemes theories on generation of entanglements are built on the interactions between spins and radio frequency pulses. In this area special spin entangled states have been prepared [26, 27] and entangled states can be also created and studied by means of nuclear-magnetic-resonance(NMR) methods [28].

It is widely believed that a quantum computer can solve some problems faster

than classical computer. Many classical algorithms used in computer are based on random walks. It is therefore interesting to consider the quantum analog of classical random walk. There are a number of different types of quantum walk. Discrete time quantum walks were proposed by Aharonov et al. [29] and Meyer[30, 31, 32] and further developed by Watrous [33]. These walks rely on an auxiliary quantum system, a "quantum coin", in order to make the time steps in the walk correspond to the action of a unitary operator. Aharonov et al. [34] and Ambainis et al[35] gave the first explicitly algorithmic context for coined quantum walks. Nayak et al. [36] studied in detail the properties of quantum walk in one dimension. Farhi and Gutmann [37] introduced continuous time quantum walks in 1997. Recently Hillery et al.[38] developed a discrete-time quantum walk model which is based on an analogy to optical interferometers, and does not require a quantum coin. Quantum walks in systems with one and two absorbing walls have also been studied[39]. Two algorithmic applications of quantum walks have been proposed so far. Childs et al [40] proved that a continuous time quantum walk can find its way across a special type of graph exponentially faster than any classical algorithm. Shenvi et al. [41] demonstrated that a search algorithm based on a coined quantum walk can obtain the same quadratic speedup as Grover's search algorithm.

Methods for the implementation of the coined quantum walk on a number of different physical systems have recently been suggested. These include ion traps [42], neutral atoms trapped in an optical lattice [43], and cavity QED, in which it is the phase of the field that undergoes the walk [44]. Very recently, additional optical implementations have been proposed using either linear optical elements [45, 46] or cavities [47, 48]. In these cavity implementations the walk takes place along frequency components of the cavity field. These papers also show that an experimental quantum walk has, in fact, been carried out, though it was not interpreted as such at the time

[49].

Bennett et al. [2] first proposed a protocol for teleporting an unknown quantum state of two-state systems such as spin-$\frac{1}{2}$ particles via a classical information channel and a quantum channel built from nonlocal quantum correlation between the sender and the receiver which share a quantum entangled state. From then on, quantum teleportation has been of interest to the physics community for many years. It holds promise for many useful applications in quantum communication and quantum computing. It consists of three steps. The first step is to prepare an entangled pair of particles that is shared between sender (Alice) and receiver (Bob). The second step is a joint measurement by Alice of the unknown system and one particle of the entangled pair in a Bell basis. In the last step, classical communication from Alice to Bob allows him to reconstruct the unknown state at his end following appropriate unitary transformations. This protocol has been verified experimentally for discrete [50], as well as continuous [51], systems. Usually atomic states are considered ideal for the storage of quantum information and are used as the stationary qubits. Earlier proposals for teleporting atomic states [52] used the atoms themselves as the carriers of quantum information (the 'flying qubits'), and recently massive particle teleportation based on the Bennett *et al.* protocol was demonstrated by two groups using ions in a trap [53].

This protocol has been extended to various quantum states in a finite dimensional Hilbert space [13, 14, 54, 55, 56, 57, 58, 59, 60, 61, 62, 63, 64, 65]. Teleportation of single-photon polarization states has been carried out experimentally [66, 67, 68]. In principle, a quantum state can be teleported with arbitrary accuracy in these protocols. Another class of protocol relates to the teleportation of continuous variable quantum states. The first protocol for teleporting quantum states in an infinite-dimensional Hilbert space was suggested by Vaidman, employing the perfect correla-

tion in both position and momentum of two particles in the EPR state [69]. The two quadrature-phase components of a single-mode optical field are analogous to position and momentum of a particle. Braunstein and Kimble [70] employed quantum nonlocal correlation between quadrature-phase components of optical fields in a two-mode squeezed vacuum state as a quantum information channel and proposed a quantum optical version of teleportation of continuous variables. Based on this protocol, quantum teleportation of a coherent state of a single-mode optical field was demonstrated experimentally [71, 72, 73]. In this protocol, the ideal teleportation could be obtained only if the initial two-mode squeezed vacuum state was ideally squeezed. However this is not possible as it would require infinite amount of energy to produce ideal two-mode squeezed vacuum state. In any quantum communication channel, perhaps the most interesting states required for teleportation are those whose quantum statistical description has no classical analog. Such nonclassical states of the radiation field are described by a P-representation $P(\alpha)$ that is not positive definite over the entire complex plane. As a result of nonideal squeezing (and also nonideal homodyne detection efficiencies), the nonclassical nature of any input beam will tend to disappear in the process of teleportation in the protocol suggested in [70]. In previous studies, only certain nonclassical properties and specific kinds of input states have been considered and the resulting conditions are dependent on the nonclassical properties and the input states under consideration [74, 75]. In the very recent paper, Caves and Wodkiewicz [76] established the relation between the Wigner functions of the input and output states in the teleportation of continuous variables and showed that the Wigner function of the output state is the Q-function of the input state when $e^{-2r} = 1/2$. Based on the relation between the variances of the phase-quadrature amplitudes of the input and output states, Ralph et al [77] obtained the same conclusion.

CHAPTER II

GENERATION OF ARBITRARY TWO-QUBIT ENTANGLED STATES

A. Preparation of an arbitrary two-photon entangled state

We consider a method for creating an arbitrary entangled state between two cavity fields. We restrict ourselves to only qubit states, i.e., the only allowed values for photon numbers in the two cavities are 0 and 1. The two cavities interact with each other via interaction with a two-level atom that is resonant with the cavity fields. The atom also interacts with two other auxiliary classical field. The atom is therefore entangled with the cavity field. However a conditional measurement reduces the final state of the atom to the desired entangled cavity field state. In general the proposed method is statistical as the probability of finding the final state of the atom in a particular state can be less than unity. However we show that, by choosing the interaction times of the atom and the fields appropriately together with special choice of relative phase between the atomic dipole and the two classical fields, we can generate a wide class of entangled states with unit probability, thus leading to a deterministic outcome.

We consider a system of two high Q cavities. The field modes inside the cavities can interact with each other via interaction with a resonant two-level atom that passes sequentially through the two cavities. Our goal is the generation of the state

$$|\psi\rangle = c_{00}\,|00\rangle + c_{01}\,|01\rangle + c_{10}\,|10\rangle + c_{11}\,|11\rangle\,, \tag{2.1}$$

where c_{00}, c_{01}, c_{10} and c_{11} are arbitrary complex amplitudes of corresponding states which satisfy the normalization condition

$$|c_{00}|^2 + |c_{01}|^2 + |c_{10}|^2 + |c_{11}|^2 = 1. \tag{2.2}$$

The schematics of the system is shown in Fig. 1. Here a resonant two-level atom initially in its excited state $|a\rangle$ interacts with two classical fields in addition to the interaction with the quantized field inside the two cavities. The classical and quantum interactions, characterized by the subscripts C and Q, respectively, are given by the following time evolution matrices

$$U_C(\tau) = \begin{pmatrix} \cos(|r|\,\tau) & -ie^{i\theta}\sin(|r|\,\tau) \\ -ie^{-i\theta}\sin(|r|\,\tau) & \cos(|r|\,\tau) \end{pmatrix} \tag{2.3}$$

where τ is the interaction time of the atom with the field and $r = |r|exp(i\theta)$ is the complex Rabi frequency,

$$U_Q(\tau) = \begin{pmatrix} \cos(|g|\,\sqrt{aa^\dagger}\tau) & -iae^{i\phi}\frac{\sin(|g|\sqrt{a^\dagger a}\tau)}{\sqrt{a^\dagger a}} \\ -ia^\dagger e^{-i\phi}\frac{\sin(|g|\sqrt{aa^\dagger}\tau)}{\sqrt{aa^\dagger}} & \cos(|g|\,\sqrt{a^\dagger a}\tau) \end{pmatrix} \tag{2.4}$$

where a and $a^\dagger$ are the annihilation and creation operators for the cavity field and g is the vacuum Rabi frequency and ϕ is the relative phase between the atomic dipole and the cavity field. We assume that the radiation field in both cavities is initially

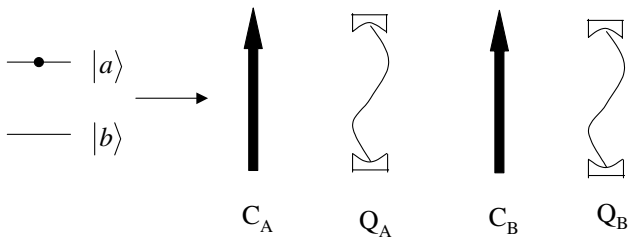

Fig. 1. Schematics for the preparation of two-mode photon states. The atom, initially in level $|a\rangle$, passes through a classical field C_A, cavity A with quantized field Q_A, classical field C_B, and finally cavity B with quantized field Q_B.

in vacuum state, i.e., the initial atom-cavity states is $|00\rangle|a\rangle$. Here $|00\rangle$ represents 0 photon in cavity A and 0 photon in cavity B.

It then follows from Eqs. (3) and (4) that the atom-field state after the atom passes through the sequence of classical and cavity fields, as shown in Fig. 1, is given by

$$\begin{aligned} |\psi_{QB}\rangle &= U_Q(\tau_{qB})U_C(\tau_{cB})U_Q(\tau_{qA})U_C(\tau_{cA})|\psi_0\rangle \\ &= (f_a[(c_a d_a e_a - c_b e_b^*)|00\rangle - c_a d_b e_b^*|10\rangle]) \otimes |a\rangle + ((c_a d_a e_b + c_b e_a)|00\rangle \\ &\quad +(c_a d_a e_a f_b - c_b e_b^* f_b)|01\rangle + c_a d_b e_a|10\rangle - c_a d_b e_b^* f_b|11\rangle) \otimes |b\rangle \end{aligned} \tag{2.5}$$

where we use the simplified notations $c_a = \cos(|r|\,\tau_{cA}) = |c_a|$, $c_b = -ie^{-i\theta_A}\sin(|r|\,\tau_{cA}) = -ie^{-i\theta_A}|c_b|$, and τ_{cA} is the time of the atom to pass through the first classical field with θ_A being the phase factor of the classical field. Similarly $d_a = \cos(|g|\,\tau_{qA}) = |d_a|$, $d_b = -ie^{-i\phi_A}\sin(|g|\,\tau_{qA}) = -ie^{-i\phi_A}|d_b|$, and τ_{qA} is the time for the atom to pass through this first cavity, with ϕ_A being the phase factor of the quantum field. Also $e_a = \cos(|r|\,\tau_{cB}) = |e_a|$, $e_b = -ie^{-i\theta_B}\sin(|r|\,\tau_{cB}) = -ie^{-i\theta_B}|e_b|$, $f_a = \cos(|g|\,\tau_{qB}) = |f_a|$, $f_b = -ie^{-i\phi_B}\sin(|g|\,\tau_{qB}) = -ie^{-i\phi_B}|f_b|$, and τ_{cB} and τ_{qB} are the times for the atom to pass through the second classical field and cavity B. As before θ_B and ϕ_B are the phase factor for the classical field and field inside cavity B.

If we make a measurement on the atom after its passage through cavity B and

the atom is found to be in the ground state, then the cavity field reduces to

$$\begin{aligned}
|\psi\rangle &= [(c_a d_a e_b + c_b e_a)\,|00\rangle + (c_a d_a e_a f_b - c_b e_b^* f_b)\,|01\rangle + c_a d_b e_a\,|10\rangle \\
&\quad -c_a d_b e_b^* f_b\,|11\rangle]/\sqrt{N} \\
&= [(-ie^{-i\theta_B})(|c_a d_a e_b| + |c_b e_a|\,e^{-i(\theta_A-\theta_B)})\,|00\rangle \\
&\quad +(-ie^{-i\phi_B})(|c_a d_a e_a f_b| - |c_b e_b f_b|\,e^{-i(\theta_A-\theta_B)}))\,|01\rangle + (-ie^{-i\phi_A})\,|c_a d_b e_a|\,|10\rangle \\
&\quad +(-ie^{-i(\phi_A+\phi_B-\theta_B)})\,|c_a d_b e_b f_b|\,|11\rangle]/\sqrt{N}. \qquad (2.6)
\end{aligned}$$

On comparing with Eq. (2.1), we have

$$\begin{aligned}
c_{00} &= (-ie^{-i\theta_B})(|c_a d_a e_b| + |c_b e_a|\,e^{-i(\theta_A-\theta_B)})/\sqrt{N}, \\
c_{01} &= (-ie^{-i\phi_B})(|c_a d_a e_a f_b| - |c_b e_b f_b|\,e^{-i(\theta_A-\theta_B)})/\sqrt{N}, \\
c_{10} &= (-ie^{-i\phi_A})\,|c_a d_b e_a|\,/\sqrt{N}, \\
c_{11} &= (-ie^{-i(\phi_A+\phi_B-\theta_B)})\,|c_a d_b e_b f_b|\,/\sqrt{N}.
\end{aligned} \qquad (2.7)$$

Here $c_{00}, c_{01}, c_{10}, c_{11}$ are the normalized amplitudes of the corresponding photon states and $N = |c_a d_a e_b + c_b e_a|^2 + |c_a d_b e_a|^2 + |c_a d_a e_a f_b - c_b e_b^* f_b|^2 + |c_a d_b e_b^* f_b|^2$ is the normalization factor.

The controlling parameters are the interaction times τ_{cA}, τ_{qA}, τ_{cB} and τ_{qB}. An arbitrary set of amplitudes c_{00}, c_{01}, c_{10}, and c_{11} can be obtained by an appropriate choice of these interaction times corresponding to a choice of c_a, d_a, e_a, and f_a. The amplitudes c_{ij} (i,j=0 or 1) are constrained by the condition $0 \leq |c_{ij}| \leq 1$. Also we have $0 \leq |c_a|, |d_a|, |e_a|, |f_a| \leq 1$. We would now like to address the question whether suitable interaction times and the phases can be found for any arbitrary set of amplitudes c_{ij}.

In general, we can find numerically a suitable choice of interaction times and

phases to generate any arbitrary state of the form (2.1). For example, the choice $\theta_A - \theta_B = 0$ can lead to the generation of any state of the form (2.1) with unit probability apart from a phase as discussed below. Our emphasis here is to give analytic expressions for the interaction parameters.

We consider two special cases ($\theta_A - \theta_B = \pi/2$ and $\theta_A - \theta_B = 0$) in the following. It is clear from Eq. (2.7) that, for these choices of $\theta_A - \theta_B$, we cover all possible set of amplitudes c_{ij} except for a phase, i.e., the phase factor associated with the state $|1,1\rangle$ is not independent. A quantum phase gate with an arbitrary phase shift can lead to an independent phase for the state $|1,1\rangle$. We shall not address the question of the generation of such a phase gate here.

1. $\theta_A - \theta_B = \pi/2$

It follows from Eq. (2.7) that

$$\begin{aligned} x_1 &= (|c_a d_a e_b|^2 + |c_b e_a|^2)/N \\ x_2 &= (|c_a d_a e_a f_b|^2 + |c_b e_b f_b)|^2 /N \\ x_3 &= |c_a d_b e_a|^2 /N \\ x_4 &= |c_a d_b e_b f_b|^2 /N, \end{aligned} \tag{2.8}$$

where $x_1 = |c_{00}|^2$, $x_2 = |c_{01}|^2$, $x_3 = |c_{10}|^2$, and $x_4 = |c_{11}|^2$. These equations can be solved for the interaction times (or equivalently for c_a, d_a, e_a and f_a).

We can rewrite Eqs. (2.8) as

$$x_i = y_i/N \tag{2.9}$$

for $i = 1 - 4$. Here the normalization constant $N = y_1 + y_2 + y_3 + y_4$. A solution of

Eq. (2.9) is given by

$$y_i = Px_i, \tag{2.10}$$

where P is a constant. Thus Eq.(2.8) reduces to

$$\begin{aligned} y_1 &= |c_a|^2|d_a|^2(1-|e_a|^2) + |e_a|^2(1-|c_a|^2) \\ y_2 &= (|c_a|^2|d_a|^2|e_a|^2 + (1-|c_a|^2)(1-|e_a|^2))(1-|f_a|^2) \\ y_3 &= |c_a|^2(1-|d_a|^2)|e_a|^2 \\ y_4 &= |c_a|^2(1-|d_a|^2)(1-|e_a|^2)(1-|f_a|^2). \end{aligned} \tag{2.11}$$

By solving this equation we can get a solution of Eq. (2.8). It is clear from the definition of P that $P = N = y_1 + y_2 + y_3 + y_4$ is the probability for the atom being in the ground state.

The solution of Eq. (8) together with the definition of x_i is given by

$$\begin{aligned} |c_a|^2 &= (Px_3x_2^2 - P^2x_1x_3x_2^2 - Px_1x_2x_4 + P^2x_1^2x_2x_4 + Px_3x_2x_4 + P^2x_3^2x_2x_4 \\ &\quad -x_4^2 + Px_1x_4^2 + 2Px_3x_4^2 - P^2x_1x_3x_4^2) \\ &\quad /[(x_2+x_4)(Px_3x_2 - x_4 + Px_1x_4 + 2Px_3x_4)] \\ |d_a|^2 &= (Px_3x_2^2 - P^2x_1x_3x_2^2 - P^2x_3^2x_2^2 - Px_1x_2x_4 + P^2x_1^2x_2x_4 + Px_3x_2x_4 \\ &\quad -P^2x_3^2x_2x_4 - Px_1x_4^2 + P^2x_1^2x_4^2 + P^2x_1x_3x_4^2)/(Px_3x_2^2 - P^2x_1x_3x_2^2 \\ &\quad -Px_1x_2x_4 + P^2x_1^2x_2x_4 + Px_3x_2x_4 + P^2x_3^2x_2x_4 \\ &\quad -x_4^2 + Px_1x_4^2 + 2Px_3x_4^2 - P^2x_1x_3x_4^2) \\ |e_a|^2 &= x_3(Px_2 + Px_4)/(Px_3x_2 + x_4 - Px_1x_4) \\ |f_a|^2 &= (-1+P)/(-1+Px_1+Px_2). \end{aligned} \tag{2.12}$$

Here $0 < P \leq 1$ with $P = 1$ corresponding to a deterministic preparation of the desired state. There are infinite number of solutions of Eq. (9) corresponding to different values of P but we would like to get a solution with maximum allowed value of $P = 1$.

However for P=1, We can not find the solution for $|c_a|^2$, $|d_a|^2$, $|e_a|^2$, $|f_a|^2$ in the range between 0 and 1 for x_i $(i = 1, 2, 3, 4)$ being also in the range 0 and 1 under following conditions.

(a) First we show that the solution (9) is not allowed when $x_1 = 0$ and $x_2x_3x_4 \neq 0$. Under these conditions, we obtain

$$|c_a|^2 = 1 + \frac{x_2x_4(1-x_3)^2}{x_3x_2^2 - x_2x_4 + 3x_3x_2x_4 - x_4^2 + 2x_3x_4^2} \tag{2.13}$$

In order for $0 \leq |c_a|^2 \leq 1$, the denominator in the second term of Eq. (2.13) must be < 0 when $x_2x_4 \neq 0$. Thus the numerator of $|c_a|^2$ in Eq. (9) should also be < 0 when $x_1 = 0$. Now the numerator of $|c_a|^2$ is equal to the denominator of $|d_a|^2$ in Eq. (9). Therefore the numerator of $|d_a|^2$ in Eq. (9) will also be < 0 when $x_1 = 0$, i.e., $x_3x_2^2 - x_3^2x_2^2 + x_3x_2x_4 - x_3^2x_2x_4 < 0$. This gives $x_3 > 1$, which is not possible.

(b) Next we show that the solution (9) is not allowed when $x_2 = 0$ and $x_1x_3x_4 \neq 0$. It follows from Eq.(9) that, under these conditions,

$$|c_a|^2 = 1 + \frac{x_1x_3}{1 - x_1 + 2x_3} \tag{2.14}$$

Now if $x_1x_3x_4 \neq 0$, we have $|c_a|^2 > 1$ for p=1 and therefore there is no allowed solution.

(c) It is also obvious that if x_1, x_2, x_3, x_4 make the denominators in $|c_a|^2$ or $|d_a|^2 = 0$ (thus leading to pole points in four dimensional space generated by x_1, x_2, x_3, x_4)

then those states are not available. For P=1 if reasonable solutions of Eq. (9) could be found numerically then x_1, x_2, x_3, x_4 are not near pole points. We note that the denominator of $|e_a|^2 \neq 0$ as x_4 is always greater than $x_1 x_4$. Also the denominator of $|f_a|^2 = 0$ only when $P = 1$ and $x_1 + x_2 = 0$, so that $x_3 = x_4 = 0$ which have trivial solutions. In summary, when x_1, x_2, x_3, x_4 are near the pole points, we obtain $|c_a|^2$ or $|d_a|^2 < 0$ or > 1 when P=1. These are therefore not possible states when $\theta_A - \theta_B = \pi/2$.

We next study the case $\theta_A - \theta_B = 0$ and find out now we can get reasonable solutions for $|c_a|^2$, $|d_a|^2$, $|e_a|^2$, $|f_a|^2$ in the range between 0 and 1 for $0 \leq x_i \leq 1$ ($i = 1, 2, 3, 4$) under conditions we talked above which we can not get suitable solutions when we choose $\theta_A - \theta_B = \pi/2$.

2. $\theta_A - \theta_B = 0$

It follows from Eq.(2.7) that

$$\begin{aligned} x_1 &= \left||c_a d_a e_b| + |c_b e_a|\right|^2 / N \\ x_2 &= \left||c_a d_a e_a f_b| - |c_b e_b f_b|\right|^2 / N \\ x_3 &= |c_a d_b e_a|^2 / N \\ x_4 &= |c_a d_b e_b f_b|^2 / N. \end{aligned} \tag{2.15}$$

A general analytic solution of $|c_a|^2$, $|d_a|^2$, $|e_a|^2$, and $|f_a|^2$ in terms of x_i ($i = 1 - 4$) is difficult. We have however seen numerically that any arbitrary state (apart from a phase in Eq. (2.7) can be generated when $\theta_A - \theta_B = 0$ with unit probability. Here we discuss some special cases where analytic results are obtained.

(i) For $x_1 = 0$ and $x_2 x_3 x_4 \neq 0$ we have

$$\begin{aligned} 0 &= |c_a|^2|d_a|^2(1-|e_a|^2) - |e_a|^2(1-|c_a|^2) \\ Px_2 &= (1-|c_a|^2)(1-|f_a|^2)/(1-|e_a|^2) \\ Px_3 &= |c_a|^2(1-|d_a|^2)|e_a|^2 \\ Px_4 &= |c_a|^2(1-|d_a|^2)(1-|e_a|^2)(1-|f_a|^2) \end{aligned} \tag{2.16}$$

These equations can be solved and the resulting expressions for the interaction parameters are

$$\begin{aligned} |c_a|^2 &= (x_4^2 + x_2^2 x_3 P + 3x_2 x_3 x_4 P - x_2 x_3^2 x_4 P^2)/[(x_2+x_4)(x_4+x_2x_3P)] \\ |d_a|^2 &= (x_2^2 x_3 P + x_2 x_3 x_4 P - x_2^2 x_3^2 P^2 - x_2 x_3^2 x_4 P^2) \\ &\quad /(x_4^2 + x_2^2 x_3 P + 3x_2 x_3 x_4 P - x_2 x_3^2 x_4 P^2) \\ |e_a|^2 &= \frac{1}{x_2+x_4}\left[-x_4 + x_3 x_4 P + \frac{1}{(x_2+x_4)(x_4+x_2x_3P)}(x_2 x_4^2 + x_4^3 + x_2^3 x_3 P \right. \\ &\quad \left. + 4x_2^2 x_3 x_4 P + 3x_2 x_3 x_4^2 P - x_2^2 x_3^2 x_4 P^2 - x_2 x_3^2 x_4^2 P^2)\right] \\ |f_a|^2 &= 1 - x_2 P - x_4 P \left\{1 - \frac{1}{x_2+x_4}\left[-x_4 + x_3 x_4 P \right.\right. \\ &\quad + \frac{1}{(x_2+x_4)(x_4+x_2x_3P)}(x_2 x_4^2 + x_4^3 + x_2^3 x_3 P + 4x_2^2 x_3 x_4 P \\ &\quad \left.\left. + 3x_2 x_3 x_4^2 P - x_2^2 x_3^2 x_4 P^2 - x_2 x_3^2 x_4^2 P^2)\right]\right\}^{-1} \end{aligned} \tag{2.17}$$

where, as before, P is the probability for the atom to be finally in the ground state.

(ii) For $x_2 = 0$ and$x_1 x_3 x_4 \neq 0$, we can see from Eq. (2.15) that if $x_4 \neq 0$ then

$|f_b|^2 \neq 0$. We have:

$$\begin{aligned} Px_1 &= (1-|c_a|^2)/|e_a|^2 \\ 0 &= |c_a d_a e_a|^2 - (1-|c_a|^2)(1-|e_a|^2) \\ Px_3 &= |c_a|^2(1-|d_a|^2)|e_a|^2 \\ Px_4 &= |c_a|^2(1-|d_a|^2)(1-|e_a|^2)(1-|f_a|^2) \end{aligned} \tag{2.18}$$

A solution of these equations is given by

$$\begin{aligned} |c_a|^2 &= (1-x_1P-x_1x_3P^2)/(1-x_1P) \\ |d_a|^2 &= x_1P(1-x_1P-x_3P)/(1-x_1P-x_1x_3P^2) \\ |e_a|^2 &= x_3P/(1-x_1P) \\ |f_a|^2 &= (1-P)/(1-P+x_4P) \end{aligned} \tag{2.19}$$

We can then see that, when $x_1 = 0$ or $x_2 = 0$ and $P = 1$, there is always a solution to satisfy $0 \leq x_1, x_2, x_3, x_4 \leq 1$ which means we can always make those states available.

(iii)Numerically we can also get reasonable solution for $|c_a|^2$, $|d_a|^2$, $|e_a|^2$, $|f_a|^2$ in the range between 0 and 1 for $0 \leq x_i \leq 1$ $(i = 1, 2, 3, 4)$ when x_1, x_2, x_3, x_4 are near pole points and p=1.

B. Generation of arbitrary two-qubit entangled atomic states

In this section we present a method to generate arbitrary entangled two-atom states based on the dipole-dipole interaction between the atoms, which gives rise to a collective state system. The key idea then is to subsequently apply driving fields to transitions in the collective state system of the two atoms. By carefully controlling the interaction times and phases of the classical driving fields, arbitrary entangled states between the two atoms can be created. Our model system consists of two nearby two-level atoms. Due to the small distance, dipole-dipole interactions gives rise to a collective state system. First, we introduce our model system, and then proceed to discuss how to address each of the transitions in this collective state system with classical fields individually. The Hamiltonian describing N two-level atoms interacting with the vacuum field can be written as [78, 79]:

$$\begin{aligned}\hat{H} = &\sum_{i=1}^{N} \hbar\omega_i S_i^z + \sum_{ks} \hbar\omega_k (\hat{a}_{ks}^\dagger \hat{a}_{ks} + \frac{1}{2}) \\ &- i\hbar \sum_{ks} \sum_{i=1}^{N} [g_{ks}(\vec{r}_i)\, S_i^+ \hat{a}_{ks} - \text{h.c.}]\,. \end{aligned} \tag{2.20}$$

Each atom consists of upper level $|a_i\rangle$ and lower level $|b_i\rangle$ with energy difference $\hbar\omega_i$ ($i \in \{1 \ldots N\}$). The single-atom operators are defined as $S_i^z = (|a_i\rangle\langle a_i| - |b_i\rangle\langle b_i|)/2$, $S_i^+ = |a_i\rangle\langle b_i|$ and $S_i^- = |b_i\rangle\langle a_i|$. $\hat{a}_{ks}$ is the annihilation operator of the vacuum field mode ks with g_{ks} as coupling constant. Using the master equation approach, the time evolution of the reduced density operator $\hat{\rho}$ for the atoms alone can be written as

$$\begin{aligned}\frac{\partial}{\partial t}\hat{\rho} \;=\; &\frac{1}{i\hbar}[\hat{H}_{aa}, \hat{\rho}] - \frac{1}{2}\sum_{i,j=1}^{N} \Gamma_{ij} \left(\hat{\rho} S_i^+ S_j^- \right. \\ &\left. + S_i^+ S_j^- \hat{\rho} - 2 S_j^- \hat{\rho} S_i^+\right)\,. \end{aligned} \tag{2.21}$$

Here, $\Gamma_{ij} = \sqrt{\Gamma_i \Gamma_j} F(k_0 r_{ij})$, where Γ_i is the spontaneous decay rate of atom i. $F(k_0 r_{ij})$ is a function of the relative position of two atoms i, j at positions $\vec{r}_i$ and $\vec{r}_j$, respectively, with $\vec{r}_{ij} = \vec{r}_i - \vec{r}_j$, $r_{ij} = |\vec{r}_i - \vec{r}_j|$ and $\bar{r}_{ij} = \vec{r}_{ij}/r_{ij}$, $k_0 = \frac{\omega_0}{c}$, and $\omega_0 = (\omega_i + \omega_j)/c$. Γ_{ij} also depends on the unit vectors $\bar{\mu} = \bar{\mu}_i = \bar{\mu}_j$ of the individual atomic dipole moments, which in the following are assumed to be equal.

The coherent evolution is governed by the Hamiltonian

$$\hat{H}_{aa} = \hbar \sum_{i=1}^{N} \omega_i S_i^z + \hbar \sum_{i \neq j} \Omega_{ij}^{dd} S_i^+ S_j^- \,. \tag{2.22}$$

The second part in Eq. (2.22) is the dipole-dipole interaction between the atoms, where Ω_{ij}^{dd} is the dipole-dipole coupling constant given by

$$\begin{aligned} \Omega_{ij}^{dd} = \frac{3}{4} \sqrt{\Gamma_i \Gamma_j} \Bigg(& - \left[1 - (\bar{\mu}.\bar{r}_{ij})^2\right] \frac{\cos(k_0 r_{ij})}{k_0 r_{ij}} \\ & + \left[1 - 3(\bar{\mu}.\bar{r}_{ij})^2\right] \left[\frac{\sin(k_0 r_{ij})}{(k_0 r_{ij})^2} + \frac{\cos(k_0 r_{ij})}{(k_0 r_{ij})^3}\right] \Bigg) \,. \end{aligned} \tag{2.23}$$

Assuming $k_0 r_{ij} \ll 1$, we have $\Gamma_{ij} \approx \sqrt{\Gamma_i \Gamma_j}$ and $\Omega_{ij}^{dd} \approx (3\sqrt{\Gamma_i \Gamma_j})/(4(k_0 r_{ij})^3)[1 - 3(\bar{\mu}.\bar{r}_{ij})^2]$, such that $\Omega_{ij}^{dd} \gg \Gamma_{ij}$ will be satisfied. Thus, in the following, we neglect the spontaneous decay of the system states.

We now focus on two interacting two-level atoms with ground states $|b_1\rangle$, $|b_2\rangle$ and excited states $|a_1\rangle$, $|a_2\rangle$. The resonance frequencies of the two atoms are ω_1 and ω_2. In the absence of dipole-dipole interaction and driving fields, the state space of the two-atom system is spanned by four product states:

$$|b_1 b_2\rangle \,, |b_1 a_2\rangle \,, |a_1 b_2\rangle \,, |a_1 a_2\rangle \,. \tag{2.24}$$

The corresponding eigenenergies are given by $E_{b_1 b_2} = -\hbar\omega_0$, $E_{a_1 b_2} = -\hbar\Delta$, $E_{b_1 a_2} = \hbar\Delta$, $E_{a_1 a_2} = \hbar\omega_0$, where $\omega_0 = \frac{1}{2}(\omega_1 + \omega_2)$ and $\Delta = \frac{1}{2}(\omega_2 - \omega_1)$. We can rewrite the two-atom interaction Hamiltonian in the matrix form (in the basis of Eq. (2.47)),

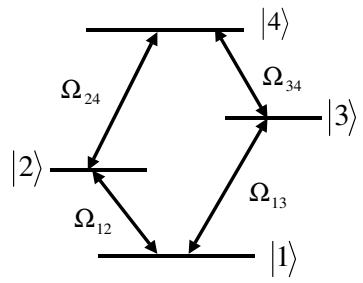

Fig. 2. Level scheme of the collective state system of two dipole-dipole interacting atoms. Such a quantum system can be described as a four-level system $|1\rangle$, $|2\rangle$, $|3\rangle$ and $|4\rangle$ in closed-loop configuration. Ω_{12}, Ω_{13}, Ω_{24} and Ω_{34} are Rabi frequencies for each of the transitions. An implementation of the individual addressing is discussed in the text.

assuming the dipole-dipole coupling constants to be same, i.e., $\Omega_{12}^{dd} = \Omega_{21}^{dd} =: \Omega$, and the two atoms to be nonidentical ($\Delta \neq 0$). It follows, on diagonalizing the matrix, that the eigenstates of this system are:

$$|1\rangle = |b_1 b_2\rangle \,, \tag{2.25a}$$

$$|2\rangle = \frac{1}{\sqrt{2}} \left(\alpha_1 |a_1 b_2\rangle - \alpha_2 |b_1 a_2\rangle\right) \,, \tag{2.25b}$$

$$|3\rangle = \frac{1}{\sqrt{2}} \left(\alpha_2 |a_1 b_2\rangle + \alpha_1 |b_1 a_2\rangle\right) \,, \tag{2.25c}$$

$$|4\rangle = |a_1 a_2\rangle \,. \tag{2.25d}$$

Here, $\alpha_1 = (1+\Delta/\sqrt{\Delta^2+\Omega^2})^{1/2}$, $\alpha_2 = (1-\Delta/\sqrt{\Delta^2+\Omega^2})^{1/2}$, and corresponding eigenenergies are:$E_1 = -\hbar\omega_0$, $E_2 = -\hbar\sqrt{\Delta^2+\Omega^2}$, $E_3 = \hbar\sqrt{\Delta^2+\Omega^2}$, $E_4 = \hbar\omega_0$.

The eigenstates Eq. (2.49) are the collective states of two interacting atoms. In this representation, the two-atom system behaves as a closed-loop single four-level system (see Fig. 2). The splitting between the two intermediate levels increases with the coupling constant Ω or the frequency difference 2Δ between the transitions of the two atoms.

Next, we discuss how to address the four transitions between the collective states Eq. (2.49) individually, i.e., how to add four driving fields labeled with Rabi frequencies of Ω_{12}, Ω_{24}, Ω_{34} and Ω_{13} separately. To distinguish between Ω_{12} and Ω_{24} (or between Ω_{34} and Ω_{13}) is possible due to the different transition frequencies, but distinguishing Ω_{12} and Ω_{34} (or Ω_{24} and Ω_{13}) requires more effort. One way to achieve the individual addressing is as follows: We align the two dipole moments of the atoms e.g. using a static magnetic or electric field. Possible energy shifts to the system states can be included by a redefinition of ω_0 and Δ. Then, the driving fields are applied to the two atoms. The classical field can be two classical fields driving each atom individually at same time or one field with a gradient in space. From the definition of the Rabi frequency we have:

$$\begin{aligned} \Omega_{12} &= \frac{\vec{E}}{\hbar} \cdot \langle 2| \left(\vec{\mu}_1 + \vec{\mu}_2\right) |1\rangle \\ &= \alpha_1 \vec{E}(\vec{r}_1) \cdot \vec{\mu}_{1ab} - \alpha_2 \vec{E}(\vec{r}_2) \cdot \vec{\mu}_{2ab}\,, \end{aligned} \tag{2.26}$$

where $\vec{\mu}_1$, $\vec{\mu}_2$ are dipole moment operators for atom 1 and 2 and $\vec{\mu}_{1ab}$, $\vec{\mu}_{2ab}$ are matrix elements of the dipole moment for atom 1 and 2 given by $\vec{\mu}_{1ab} = \langle a_1| \vec{\mu_1} |b_1\rangle$, $\vec{\mu}_{2ab} = \langle a_2| \vec{\mu_2} |b_2\rangle$. Similarly, we have

$$\begin{aligned} \Omega_{34} &= \frac{\vec{E}}{\hbar} \cdot \langle 4| \left(\vec{\mu_1} + \vec{\mu_2}\right) |3\rangle \\ &= \alpha_1 \vec{E}(\vec{r}_1) \cdot \vec{\mu}_{1ab} + \alpha_2 \vec{E}(\vec{r}_2) \cdot \vec{\mu}_{2ab}\,. \end{aligned} \tag{2.27}$$

When the driving field satisfies $\alpha_1 \vec{E}(\vec{r}_1) \cdot \vec{\mu}_{1ab} = \alpha_2 \vec{E}(\vec{r}_2) \cdot \vec{\mu}_{2ab}$, one obtains $\Omega_{12} = 0$, but $\Omega_{34} \neq 0$. Thus the driving field selectively drives the $|3\rangle \leftrightarrow |4\rangle$ transition only. On the other hand, if we choose the driving field such that $\alpha_1 \vec{E}(\vec{r}_1) \cdot \vec{\mu}_{1ab} = -\alpha_2 \vec{E}(\vec{r}_2) \cdot \vec{\mu}_{2ab}$, then $\Omega_{34} = 0$, but $\Omega_{12} \neq 0$, and the other transition is driven. An analogous scheme is possible for the transitions $|1\rangle \leftrightarrow |3\rangle$ and $|2\rangle \leftrightarrow |4\rangle$. Thus each of the four transitions

can be addressed separately.

Our main goal is to propose a scheme for the generation of an arbitrary superposition of the atomic states, i.e.,

$$\begin{aligned} |\psi\rangle &= c_{b_1b_2}\,|b_1b_2\rangle + c_{b_1a_2}\,|b_1a_2\rangle \\ &\quad + c_{a_1b_2}\,|a_1b_2\rangle + c_{a_1a_2}\,|a_1a_2\rangle\ , \end{aligned} \tag{2.28}$$

where $c_{b_1b_2}$, $c_{b_1a_2}$, $c_{a_1b_2}$ and $c_{a_1a_2}$ are arbitrary complex amplitudes of the corresponding states, which satisfy the normalization condition

$$|c_{b_1b_2}|^2 + |c_{b_1a_2}|^2 + |c_{a_1b_2}|^2 + |c_{a_1a_2}|^2 = 1\,. \tag{2.29}$$

We now show how, by subsequently driving transitions $|1\rangle \leftrightarrow |2\rangle$, $|2\rangle \leftrightarrow |4\rangle$ and $|3\rangle \leftrightarrow |4\rangle$ with tailored classical fields, we can generate an arbitrary two qubit atomic state of the form Eq. (2.51). First, we note that the state Eq. (2.51) in the bare basis Eq. (2.47) is equivalent to

$$|\psi\rangle = c_1\,|1\rangle + c_2\,|2\rangle + c_3\,|3\rangle + c_4\,|4\rangle \tag{2.30}$$

in the dipole-dipole interaction basis (see Eq. (2.49)) with

$$c_1 = c_{b_1b_2}\,, \tag{2.31a}$$

$$c_2 = \frac{1}{\sqrt{2}}\left(-\alpha_2 c_{b_1a_2} + \alpha_1 c_{a_1b_2}\right)\,, \tag{2.31b}$$

$$c_3 = \frac{1}{\sqrt{2}}\left(\alpha_1 c_{b_1a_2} + \alpha_2 c_{a_1b_2}\right)\,, \tag{2.31c}$$

$$c_4 = c_{a_1a_2}\,. \tag{2.31d}$$

It is well known that one can obtain an arbitrary superposition state of a single two-level atom by using a pulsed driving field between the two levels. This motivates us to apply similar techniques to obtain an arbitrary superposition state of the four

collective states by applying classical fields between the four levels. Consider a two-state system $\{|i\rangle, |j\rangle\}$, labeled by subindices ij. The interaction Hamiltonian of this system with a classical field is [19]

$$V_{ij} = -\hbar\Omega_{ij} |j\rangle \langle i| + \text{ h.c.}. \tag{2.32}$$

The time evolution operator in the basis of levels $|i\rangle$ and $|j\rangle$ can be written as [19]:

$$U_C^{(k)} = \begin{pmatrix} \cos(|\Omega_{ij}|\, t_k) & -ie^{i\Phi_k}\sin(|\Omega_{ij}|\, t_k) \\ -ie^{-i\Phi_k}\sin(|\Omega_{ij}|\, t_k) & \cos(|\Omega_{ij}|\, t_k) \end{pmatrix}. \tag{2.33}$$

In the following, we apply these two-level time evolutions to the transitions $ij \in \{12, 24, 34\}$, where k labels the step in the sequence of applied driving fields.

The generation of arbitrary two-atom states involves three steps. Initially, the two atoms assumed to be in the ground state $|1\rangle$. In the first step, a driving field is applied between the levels $|1\rangle$ and $|2\rangle$ for a duration t_1 with coupling $\Omega_{12} = |\Omega_{12}|\, e^{i\Phi_1}$. The interaction Hamiltonian is V_{12} and the time evolution operator is $U_C^{(1)}$. After time t_1 the system states is:

$$|\psi(t_1)\rangle = c_1(t_1)\,|1\rangle + c_2(t_1)\,|2\rangle\ , \tag{2.34}$$

where the state amplitudes are given by

$$c_1(t_1) = \cos(|\Omega_{12}|\, t_1)\,, \tag{2.35}$$

$$c_2(t_1) = -ie^{i\Phi_1 + i\nu_1 t_1}\ \sin(|\Omega_{12}|\, t_1)\,, \tag{2.36}$$

with $\nu_1 = (E_2 - E_1)/\hbar$. The overall phase factor $\exp[i/\hbar\, E_1 t_1]$ is omitted here. We choose the interaction time t_1 such that $\cos(|\Omega_{12}|\, t_1) = c_1$. The phase Φ_1 will be chosen in the final step. The system state at the end of the first step can then be

written as

$$|\psi(t_1)\rangle = c_1\,|1\rangle + c_2(t_1)\,|2\rangle\ . \tag{2.37}$$

In next step the driving field between $|2\rangle$ and $|4\rangle$ is turned on for a duration t_2 with coupling strength $\Omega_{24} = |\Omega_{24}|\exp[i\Phi_2]$. As before, the interaction Hamiltonian can be written as V_{24} and the time evolution operator is $U_C^{(2)}$. At the end of the pulse duration t_2, the system has evolved to

$$|\psi(t_2)\rangle = c_1\,|1\rangle + c_2(t_2)\,|2\rangle + c_4(t_2)\,|4\rangle\ , \tag{2.38}$$

where

$$\begin{aligned} c_2(t_2) &= \cos(|\Omega_{24}|\,t_2)e^{i\nu_1 t_2}\,c_2(t_1) \\ &= -i\cos(|\Omega_{24}|\,t_2)\,\sin(|\Omega_{12}|\,t_1) \\ &\quad \times e^{i(\nu_1(t_1+t_2)+\Phi_1)}\,, \end{aligned} \tag{2.39}$$

$$\begin{aligned} c_4(t_2) &= -i\,e^{i(\nu_1+\nu_2)t_2+i\Phi_2}\,\sin(|\Omega_{24}|\,t_2)\,c_2(t_1) \\ &= -\sin(|\Omega_{24}|\,t_2)\,\sin(|\Omega_{12}|\,t_1) \\ &\quad \times e^{i(\nu_1 t_1+(\nu_1+\nu_2)t_2+\Phi_1+\Phi_2)}\,, \end{aligned} \tag{2.40}$$

and $\nu_2 = (E_4 - E_2)/\hbar$. The overall phase factor $\exp[iE_1t_2/\hbar]$ is omitted as before.

Finally, a field between $|4\rangle$ and $|3\rangle$ is applied for the duration t_3 with Rabi frequency $\Omega_{34} = |\Omega_{34}|\exp[i\Phi_3]$. The interaction Hamiltonian can be written as V_{34} and the time evolution operator is $U_C^{(3)}$. The atomic system evolves to the state

$$|\psi(t_3)\rangle = c_1\,|1\rangle + c_2(t_3)\,|2\rangle + c_4(t_3)\,|4\rangle + c_3(t_3)\,|3\rangle\ , \tag{2.41}$$

where

$$c_2(t_3) = -i\cos(|\Omega_{24}|\,t_2)\,\sin(|\Omega_{12}|\,t_1)e^{i(\Phi_1+\nu_1(t_1+t_2+t_3))}\,,$$

with overall phase factor $\exp[i/\hbar E_1 t_3]$ omitted. We can see that by choosing the interaction time t_2 in the second step and the phase Φ_1 in the first step appropriately, we can obtain $c_2(t_3) = c_2$. The amplitude of state $|4\rangle$ then is

$$\begin{aligned} c_4(t_3) &= \cos(|\Omega_{34}|\, t_3)\, e^{i(\nu_1+\nu_2)t_3} c_4(t_2) \\ &= -\cos(|\Omega_{34}|\, t_3)\, \sin(|\Omega_{24}|\, t_2)\, \sin(|\Omega_{12}|\, t_1) \\ &\quad \times e^{i[(\nu_1+\nu_2)(t_2+t_3)+\nu_1 t_1+\Phi_1+\Phi_2]} \end{aligned} \tag{2.42}$$

and, by choosing interaction time t_3 and Φ_2 appropriately, $c_4(t_3) = c_4$ can be satisfied. With these parameter choices, the amplitude of state $|3\rangle$ becomes

$$\begin{aligned} c_3(t_3) &= -ie^{i\nu_3 t_3 + i\Phi_3}\, \sin(|\Omega_{34}|\, t_3) c_4(t_2) \\ &= i \sin(|\Omega_{34}|\, t_3) \sin(|\Omega_{24}|\, t_2) \sin(|\Omega_{12}|\, t_1) \\ &\quad \times e^{i[\nu_1 t_1+(\nu_1+\nu_2)t_2+\nu_3 t_3+\Phi_1+\Phi_2-\Phi_3]}\,, \end{aligned} \tag{2.43}$$

where $\nu_3 = (E_3 - E_1)/\hbar$. Upon simplification of the above expression, it follows that $|c_3(t_3)| = |c_3|$ automatically. By choosing a suitable phase Φ_3, the system state becomes the desired state given in Eq. (2.30), which is equivalent to the state Eq. (2.51).

We now proceed to give a concrete example of our scheme. Assume that we want to create a two-atoms state of the form

$$|\psi\rangle = \frac{1}{2}[|b_1 b_2\rangle + e^{i\theta_1}\,|b_1 a_2\rangle + e^{i\theta_2}\,|a_1 b_2\rangle + e^{i\theta_3}\,|a_1 a_2\rangle]\,, \tag{2.44}$$

and that the two atoms satisfy $\Delta/\Omega = 3/4$. In the collective state basis, the desired state takes form:

$$\begin{aligned} |\psi\rangle &= \frac{1}{2}\Bigg[|1\rangle + \sqrt{\frac{1}{5}}\left(-e^{i\theta_1} + 2e^{i\theta_2}\right)|2\rangle \\ &\quad + \sqrt{\frac{1}{5}}\left(2e^{i\theta_1} + e^{i\theta_2}\right)|3\rangle + e^{i\theta_3}\,|4\rangle\Bigg]\,. \end{aligned} \tag{2.45}$$

As before, we start from atomic ground states $|1\rangle$ and apply a classical field between states $|1\rangle$ and $|2\rangle$ with condition $\cos(|\Omega_{12}|\, t_1) = \frac{1}{2}$. The system state becomes

$$|\psi(t_1)\rangle = \frac{1}{2}\,|1\rangle - ie^{i(\Phi_1+\nu_1 t_1)}\sqrt{\frac{3}{4}}\,|2\rangle\ . \tag{2.46}$$

Next, a driving field of duration t_2 is applied between $|2\rangle$ and $|4\rangle$ with the condition: $\cos(|\Omega_{24}|\, t_2) = \sqrt{1/3 - 4/15\,\cos(\theta_2-\theta_1)}$. Finally, transition $|4\rangle \leftrightarrow |3\rangle$ is driven for time t_3 with the condition that $\cos(|\Omega_{34}|\, t_3) = (2 + 4/5\,\cos(\theta_2-\theta_1))^{-1/2}$. The phases of the coupling fields should be chosen as $\Phi_1 = -\nu_1(t_1+t_2+t_3) + \theta_1 + \beta_1 - \frac{\pi}{2}$, under the condition $\cos(\beta_1) = (-1 + 2\cos(\theta_2-\theta_1))/(5 - 4\cos(\theta_2-\theta_1))$. The second field phase is chosen such that $\Phi_2 = \theta_3 - \Phi_1 - \nu_2(t_2+t_3)$. The last phase is taken as $\Phi_3 = -\theta_1 + \theta_3 - \beta_2 + (\nu_3-\nu_2)t_3$ where β_2 satisfies $\cos(\beta_2) = (2+\cos(\theta_2-\theta_1))/(5 + 4\cos(\theta_2-\theta_1))$. Then the final system state is the desired state Eq. (2.45), which is identical to Eq. (2.44) in the bare basis. The time evolution of the four system state populations is shown in Fig. 3, where for simplify we choose $\theta_1 = \theta_3 = 0$, $\theta_2 = \frac{\pi}{2}$ and $\Omega_{12} = \Omega_{24} = \Omega_{34} = \Omega$. The phases and the interaction times are chosen as discussed above. From Fig. 3 we can see that starting from initial state $|1\rangle$, after step by step turning on the three driving fields, the final populations of all four basis states ends up at the same value 1/4 as desired.

It is not difficult to see that the method introduced above can be applied for any initial state. It should be noted, however, that spontaneous decay is assumed to be weak as compared to the interactions between the atoms and the driving fields in our discussion, that is, the state preparation is assumed to be fast enough such that the effect of spontaneous emission will be small. The scheme can also make use of off-resonant driving fields, and is well-suited for other two-level quantum systems such as two spin-1/2 particles, where the driving fields are radio frequency fields.

In this paper we consider only the resonance driving for one particular transition

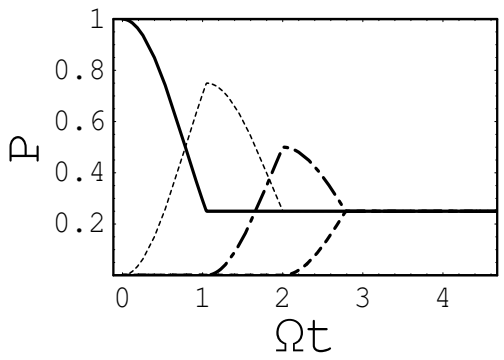

Fig. 3. Schematics for the Population dynamics of the four levels. Solid line is state $|1\rangle$, dotted line is state $|2\rangle$, dash-dotted line line is state $|4\rangle$, and dashed line is state $|3\rangle$. For simplicity, we chose $\theta_1 = \theta_3 = 0, \theta_2 = \frac{\pi}{2}$ and coupling constants $\Omega_{12} = \Omega_{24} = \Omega_{34} = \Omega$.

between two level in each step. In practice, the spectrum of the driving field is broadened due to the finite interaction-time for each the transition, and the non-resonant effect exists for particular transition. The longer the interaction time is, the sharper the spectrum of the driving field is, and the weaker the non-resonant effect becomes. The detailed discussion is more complex and will appear in another paper. In addition, if the transition frequency between$|1\rangle$ and $|2\rangle$ (or between$|3\rangle$ and $|4\rangle$) is far away from that for the levels $|2\rangle$ and $|4\rangle$ (or $|1\rangle$ and $|3\rangle$), we will see that, due to large detuning the non-resonant effect to the other transition will be neglected as we drive on a particular transition.

C. Arbitrary entangled states for two-spin system

Here we will show a method to generate arbitrary two qubit entangled spin states based on interaction between spin and radio frequency pulses in a two-spin systems. The weak interaction between the two spins leads to that the system of two spin behaves as a single four-level system with four eigenstates. We can get arbitrary

entangled two-spin states in those four states basis by adding the radio frequency pulses step by step with controlled times and phases.

Let us consider two interacting spin atoms, spin I with gyro-magnetic ratio γ_I and spin S with gyro-magnetic ratio γ_s. The directions of spins will be decided by a static magnetic field of magnitude B_0 and initially they are at rest and interact weakly with each other via a scalar coupling $AI \cdot S$, where A is coupling constant. The direction of the static magnetic field is defined as Z axis. In the absence of the weak interaction between spins, the bare state basis of the two-spin system is spanned by four product states:

$$|\downarrow\downarrow\rangle = |1\rangle\,, |\downarrow\uparrow\rangle = |2\rangle\,, |\uparrow\downarrow\rangle = |3\rangle\,, |\uparrow\uparrow\rangle = |4\rangle\,, \tag{2.47}$$

where first term of up or down arrow denotes spin states of spin S and second term denotes states of spin I.

In this paper our goal is the generation of the state.

$$|\psi\rangle = c_1\,|1\rangle + c_2\,|2\rangle + c_3\,|3\rangle + c_4\,|4\rangle\,, \tag{2.48}$$

where the coefficient c_1 is real number, and the coefficients c_2, c_3 and c_4 are arbitrary complex amplitudes of corresponding states, and satisfy the following normalization condition

$$|c_1|^2 + |c_2|^2 + |c_3|^2 + |c_4|^2 = 1. \tag{2.49}$$

When we consider the weak interaction between the two spins, the Hamiltonian of this system takes the form[27]:

$$\hat{H}_{spin} = \hbar\gamma_s B_0 S_Z + \hbar\gamma_I B_0 I_Z + A\hbar I \cdot S. \tag{2.50}$$

The static magnetic field B_0 will be strong enough so that only $AS_Z I_Z$ term is dom-

inant from the spin-spin coupling, thus Hamiltonian takes form:

$$\hat{H}_{spin} = \hbar\gamma_s B_0 S_Z + \hbar\gamma_I B_0 I_Z + A\hbar S_Z I_Z, \tag{2.51}$$

The states $|1\rangle$, $|2\rangle$, $|3\rangle$ and $|4\rangle$ are eigenstats for Hamiltonian (2.51), eigenenergies for each corresponding basis are:

$$\begin{aligned}
E_1 &= -\frac{\hbar B_0(\gamma_s+\gamma_I)}{2} + \frac{A}{4}, && \text{(2.52a)}\\
E_2 &= -\frac{\hbar B_0(\gamma_s-\gamma_I)}{2} - \frac{A}{4}, && \text{(2.52b)}\\
E_3 &= -\frac{\hbar B_0(\gamma_I-\gamma_s)}{2} - \frac{A}{4}, && \text{(2.52c)}\\
E_4 &= \frac{\hbar B_0(\gamma_s+\gamma_I)}{2} + \frac{A}{4}. && \text{(2.52d)}
\end{aligned}$$

After considering the weak interaction between the two spins, the two-spin system behaves as a closed-loop single four-level system with the ground state $|1\rangle$, the upper state $|4\rangle$, and two intermediate states $|2\rangle$ and $|3\rangle$. The Hamiltonian can be written as $\hat{H}_{spin} = \sum_{i=1}^{4} E_i |i\rangle \langle i|$. Now we consider the four level system interaction(as show in Fig. 4). Ω_{12}, Ω_{13}, Ω_{24} and Ω_{34} are corresponding interaction coupling constant between spin and four radio frequency pulses with $|\Omega_{ij}| = \gamma^{I,S} B_{ij}$ where B_{ij} are amplitudes of radio frequency pulses added between level i and j.

From Eq.(2.52) and Fig. 4, we can see that energy level separation between level $|1\rangle$ and $|2\rangle$, $|2\rangle$ and $|4\rangle$, $|3\rangle$ and $|4\rangle$, $|1\rangle$ and $|3\rangle$ are different from each others. So it is possible to distinguish the four added radio frequency pulses between four levels. It is obvious that we can obtain an arbitrary superposition state of a single two-level atom using a driving field pulse between the two levels. We will see in the following that this method in one qubit case will be used sequentially in three steps and desired two qubits entangled state in Eq.(2.48) will be produced by controlling times and phases

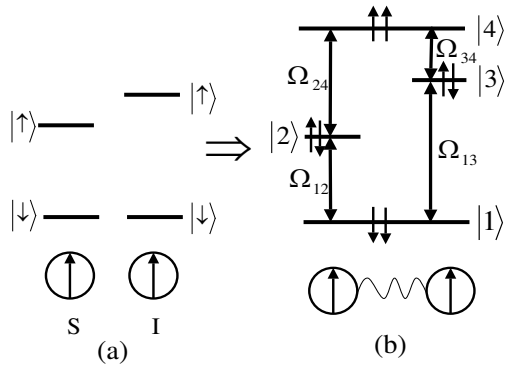

Fig. 4. (a)Two spin S and I without interaction. Each have a spin up and spin down eigenstates. (b)Schematics for the two spins with weak interaction coupled by four radio frequency. Such quantum system can be described as a four-level system in closed-loop configuration. $|1\rangle$, $|2\rangle$, $|3\rangle$ and $|4\rangle$ are four eigenstates. Ω_{12}, Ω_{13}, Ω_{24} and Ω_{34} are corresponding interaction coupling constant between spin and four radio frequency pulses.

of those radio frequency pulses between four levels.

Let's first review an atom with two-level $\{|i\rangle, |j\rangle\}$ interacting resonantly with a classical field. The Hamiltonian of this system takes the following form in the interaction picture [19].

$$V_{ij} = -\hbar\Omega_{ij} |j\rangle \langle i| + \text{ h.c.}. \tag{2.53}$$

Solving Schrödinger equation $i\hbar\frac{\partial}{\partial t}\psi_I(t) = V_{ij}\psi_I(t)$, we can get the state vector $\psi_I(t)$ in the interaction picture,

$$\psi_I(t_k) = U_C^{(k)}\psi_I(0). \tag{2.54}$$

Where $U_C^{(k)}$ is the time evolution operator in the basis of levels $|i\rangle$ and $|j\rangle$, $U_C^{(k)}$ can be written as:

$$U_C^{(k)} = \begin{pmatrix} \cos(|\Omega_{ij}|\, t_k) & -ie^{i\Phi_k}\sin(|\Omega_{ij}|\, t_k) \\ -ie^{-i\Phi_k}\sin(|\Omega_{ij}|\, t_k) & \cos(|\Omega_{ij}|\, t_k) \end{pmatrix}. \tag{2.55}$$

where $\Omega_{ij} = |\Omega_{ij}|\, e^{i\Phi_k}$, and t_k is interaction period. In the following discussion the index ij and k will be chosen as $ij = 12, 24, 34$ and $k = 1, 2, 3$ for three driving steps respectively.

The generation of arbitrary two-qubit spin state in Eq.(2.52) consists of three steps, driving radio frequency pulses labeled as Ω_{12} Ω_{24} and Ω_{34} with constant amplitudes will be added sequentially to the system, first radio frequency pulse Ω_{12} will be turned on for time t_1, second radio frequency pulse Ω_{24} will be turned on for time t_2 and finally Ω_{34} will be turned on for time t_3. After final step state in Eq.(2.52) will be generated by controlling the interaction time and the phases of the radio frequency pulses.

In first step we prepare spin state initially as $|1\rangle$, then we turn on the radio frequency pulse between $|1\rangle$ and $|2\rangle$ for time t_1 with coupling $\Omega_{12} = |\Omega_{12}|\, e^{i\Phi_1}$, the interaction Hamiltonian is V_{12} and the time evolution operator is $U_C^{(1)}$ as introduced above, after time t_1 the system states then evolves as:

$$|\psi(t_1)\rangle_I = c_{I1}(t_1)\,|1\rangle + c_{I2}(t_1)\,|2\rangle\,,$$

with

$$\begin{aligned} c_{I1}(t_1) &= \cos(|\Omega_{12}|\, t_1), \\ c_{I2}(t_1) &= -ie^{i\Phi_1}\sin(|\Omega_{12}|\, t_1). \end{aligned}$$

Thus the system state in Schrödinger picture will be written as:

$$|\psi(t_1)\rangle = c_1(t_1)\,|1\rangle + c_2(t_1)\,|2\rangle\,, \tag{2.56}$$

with

$$\begin{aligned} c_1(t_1) &= e^{-iE_1t_1/\hbar}c_{I1}(t_1) \\ &= e^{-iE_1t_1/\hbar}\cos(|\Omega_{12}|\,t_1), \\ c_2(t_1) &= e^{-iE_2t_1/\hbar}c_{I2}(t_1) \\ &= -ie^{i\Phi_1-iE_2t_1/\hbar}\sin(|\Omega_{12}|\,t_1). \end{aligned}$$

Interaction time t_1 will be chosen such that $\cos(|\Omega_{12}|\,t_1) = c_1$, and the phase term Φ_1 will satisfy the condition which can be seen in the final step.

In second step we add the radio frequency pulse between $|2\rangle$ and $|4\rangle$ for time t_2 with coupling $\Omega_{24} = |\Omega_{24}|\,e^{i\Phi_2}$. The initial state vector is described by Eq.(2.56). Simillar to the first step the interaction Hamiltonian will be written as V_{24} and the time evolution operator is $U_C^{(2)}$ which gives the system states in interaction picture after time t_2 as:

$$|\psi(t_2)\rangle_I = c_1(t_1)\,|1\rangle + c_{I2}(t_2)\,|2\rangle + c_{I4}(t_2)\,|4\rangle$$

with

$$\begin{aligned} c_{I2}(t_2) &= \cos(|\Omega_{24}|\,t_2)c_2(t_1), \\ c_{I4}(t_2) &= -ie^{i\Phi_2}\sin(|\Omega_{24}|\,t_2)c_2(t_1), \end{aligned}$$

and the state vector in Schrödinger picture can be written as:

$$|\psi(t_2)\rangle = c_1(t_2)\,|1\rangle + c_2(t_2)\,|2\rangle + c_4(t_2)\,|4\rangle \tag{2.57}$$

with

$$\begin{aligned} c_1(t_2) &= e^{-iE_1t_2/\hbar}c_1(t_1) \\ &= e^{-iE_1(t_1+t_2)/\hbar}c_1, \\ c_2(t_2) &= e^{-iE_2t_2/\hbar}c_{I2}(t_2) \\ &= -ie^{i\Phi_1-iE_2(t_1+t_2)/\hbar}\sin(|\Omega_{12}|\,t_1)\cos(|\Omega_{24}|\,t_2), \\ c_4(t_2) &= e^{-iE_4t_2/\hbar}c_{I4}(t_2) \\ &= -e^{i\Phi_1+i\Phi_2-iE_2t_1/\hbar-iE_4t_2/\hbar}\sin(|\Omega_{12}|\,t_1)\sin(|\Omega_{24}|\,t_2). \end{aligned}$$

We can choose the interaction time t_2 such that $\sin(|\Omega_{12}|\,t_1)\cos(|\Omega_{24}|\,t_2) = |c_2|$, and the phase Φ_2 will be determined later.

In last step the radio frequency pulse between $|4\rangle$ and $|3\rangle$ will be turned on for time t_3 with $\Omega_{34} = |\Omega_{34}|\,e^{i\Phi_3}$. The interaction Hamiltonian now will be written as V_{34} and the time evolution operator will be $U_C^{(3)}$. In this step the initial system state vector is represented by Eq. (2.57), and the final system states (in interaction picture) evolves to:

$$|\psi(t_3)\rangle_I = c_1(t_2)\,|1\rangle + c_2(t_2)\,|2\rangle + c_{I4}(t_3)\,|4\rangle + c_{I3}(t_3)\,|3\rangle$$

with

$$\begin{aligned} c_{I4}(t_3) &= \cos(|\Omega_{34}|\,t_3)c_4(t_2), \\ c_{I3}(t_3) &= -ie^{i\Phi_3}\sin(|\Omega_{34}|\,t_3)c_4(t_2). \end{aligned}$$

Then we can get the final state vector in Schrödinger picture:

$$|\psi(t_3)\rangle = c_1(t_3)\,|1\rangle + c_2(t_3)\,|2\rangle + c_4(t_3)\,|4\rangle + c_3(t_3)\,|3\rangle\,, \tag{2.58}$$

and the amplitudes of corresponding eigenstates, $c_1(t_3)$, $c_2(t_3)$, $c_3(t_3)$ and $c_4(t_3)$ can

be obtained.

$$\begin{aligned}
c_1(t_3) &= e^{-iE_1 t_3/\hbar} c_1(t_2) \\
&= e^{-iE_1(t_1+t_2+t_3)/\hbar} c_1, \\
c_2(t_3) &= e^{-iE_2 t_3/\hbar} c_2(t_2) \\
&= -ie^{i\Phi_1 - iE_2(t_1+t_2+t_3)/\hbar} |c_2|, \\
c_4(t_3) &= e^{-iE_4 t_3/\hbar} c_{I4}(t_2) \\
&= -\sin(|\Omega_{12}|\, t_1) \sin(|\Omega_{24}|\, t_2) \cos(|\Omega_{34}|\, t_3) \\
&\quad \times e^{i\Phi_1 + i\Phi_2 - iE_2 t_1/\hbar - iE_4 t_2/\hbar - - iE_4 t_3/\hbar}, \\
c_3(t_3) &= e^{-iE_3 t_3/\hbar} c_{I3}(t_3) \\
&= i \sin(|\Omega_{12}|\, t_1) \sin(|\Omega_{24}|\, t_2) \sin(|\Omega_{34}|\, t_3) \\
&\quad \times e^{i\Phi_1 + i\Phi_2 + i\Phi_3 - iE_2 t_1/\hbar - iE_4 t_2/\hbar - iE_3 t_3/\hbar}.
\end{aligned}$$

Choosing suitable interaction time t_3, the equation $\sin(|\Omega_{12}|\, t_1) \sin(|\Omega_{24}|\, t_2) \cos(|\Omega_{34}|\, t_3) = |c_4|$ can be satisfied. At the same time, we have $|c_3(t_3)| = |c_3|$ from the normalization condition Eq. (2.49). In the following one can see that the system state vector Eq. (2.58) will become the desired state with form of Eq (2.48) by choosing suitable phases Φ_1, Φ_2 and Φ_3.

Neglecting the common phase factor $\exp[-iE_1(t_1 + t_2 + t_3)/\hbar]$ in Eq.(2.58), the state vector can be rewritten as

$$|\psi(t_3)\rangle = c_1' |1\rangle + c_2' |2\rangle + c_3' |3\rangle + c_4' |4\rangle , \tag{2.59}$$

and the coefficients c_1', c_2', c_3' and c_4' can be obtained as following:

$$c_1' = c_1, \tag{2.60a}$$

$$c_2' = -ie^{i[\Phi_1-\nu_1(t_1+t_2+t_3)]}|c_2|, \tag{2.60b}$$

$$c_3' = \pm ie^{i[\Phi_1+\Phi_2+\Phi_3-\nu_1 t_1-(\nu_1+\nu_2)t_2-\nu_3 t_3]}|c_3|, \tag{2.60c}$$

$$c_4' = -e^{i[\Phi_1+\Phi_2-\nu_1 t_1-(\nu_1+\nu_2)(t_2+t_3)]}|c_4|, \tag{2.60d}$$

where $\nu_1 = (E_2 - E_1)/\hbar$, $\nu_2 = (E_4 - E_2)/\hbar$,and $\nu_3 = (E_3 - E_1)/\hbar$. sign(+) and sign(-) in Eq. (2.60c) are related to $P = \sin(|\Omega_{12}|\, t_1)\sin(|\Omega_{24}|\, t_2)\sin(|\Omega_{34}|\, t_3) > 0$ and $P < 0$, respectively. Supposing the complex coefficients c_2, c_3 and c_4 in Eq.(2.48) take the form of $c_2 = |c_2|\, e^{i\theta_1}$, $c_3 = |c_3|\, e^{i\theta_2}$, $c_4 = |c_4|\, e^{i\theta_3}$, we can choose the phase terms Φ_1, Φ_2 and Φ_3 such that $\theta_1 = \Phi_1 - \nu_1(t_1 + t_2 + t_3) - \pi/2$, $\theta_2 = \Phi_1 + \Phi_2 + \Phi_3 - \nu_1 t_1 - (\nu_1 + \nu_2)t_2 - \nu_3 t_3 \pm \pi/2$ (sign(+) for $P > 0$ and sign(-) for $P < 0$),and $\theta_3 = \Phi_1 + \Phi_2 - \nu_1 t_1 - (\nu_1 + \nu_2)(t_2 + t_3) - \pi$.Thus the Eq.(2.59) takes the same form of the Eq.(2.48).

In summary, to get state of Eq (2.48) the choice of the time period and phase term for each step will satisfy:

$$cos(|\Omega_{12}|\, t_1) = c_1\,, \tag{2.61a}$$

$$cos(|\Omega_{24}|\, t_2) = \frac{|c_2|}{sin(|\Omega_{12}|\, t_1)}\,, \tag{2.61b}$$

$$cos(|\Omega_{34}|\, t_3) = \frac{|c_4|}{sin(|\Omega_{24}|\, t_2)sin(|\Omega_{12}|\, t_1)}\,, \tag{2.61c}$$

$$\Phi_1 = \theta_1 + \nu_1(t_1 + t_2 + t_3) + \frac{\pi}{2}\,, \tag{2.61d}$$

$$\Phi_2 = \theta_3 - \theta_1 + \nu_2(t_2 + t_3) + \frac{\pi}{2}\,, \tag{2.61e}$$

$$\Phi_3 = \theta_2 - \theta_3 + (\nu_3 - \nu_1 - \nu_2)t_3 \pm \frac{\pi}{2}\,, \tag{2.61f}$$

where sign(+) is for $P > 0$ and sign(-) is for $P < 0$.

To illustrate the theory clearly next we give an example. If we want to create two spins state:

$$|\psi\rangle = \frac{1}{4}|1\rangle + \frac{1}{2}e^{i\frac{\pi}{2}}|2\rangle + \frac{3}{4}e^{i\pi}|3\rangle + \frac{\sqrt{2}}{4}e^{i\frac{3\pi}{2}}|4\rangle \tag{2.62}$$

We start from spin state $|1\rangle$ and turn on the radio frequency pulse between $|1\rangle$ and $|2\rangle$ with condition $cos(|\Omega_{12}|\, t_1) = \frac{1}{4}$. The system state becomes:

$$|\psi(t_1)\rangle = \frac{1}{4}|1\rangle - ie^{i(\Phi_1 - \nu_1 t_1)}\sqrt{\frac{15}{16}}|2\rangle \tag{2.63}$$

Then the radio frequency pulse between $|2\rangle$ and $|4\rangle$ with coupling $\Omega_{24} = |\Omega_{24}|\, e^{i\Phi_2}$ was turn on for time t_2 which satisfy $cos(|\Omega_{24}|\, t_2) = \sqrt{\frac{4}{15}}$, we get the system state:

$$\begin{aligned} |\psi(t_2)\rangle &= \frac{1}{4}|1\rangle - i\frac{1}{2}e^{i[\Phi_1 - \nu_1(t_1+t_2)]}|2\rangle \\ &\quad -\sqrt{\frac{11}{16}}e^{i[\Phi_1+\Phi_2-\nu_1(t_1+t_2))-\nu_2 t_2]}|4\rangle \end{aligned} \tag{2.64}$$

For the last step, we turn on only the radio frequency pulse between $|4\rangle$ and $|3\rangle$ with coupling $\Omega_{34} = |\Omega_{34}|\, e^{i\Phi_3}$ for time t_3 on the condition that $cos(|\Omega_{34}|\, t_3) = \sqrt{\frac{2}{11}}$, if only we choose phase term in each step such that: $\Phi_1 = \nu_1(t_1 + t_2 + t_3) + \pi$, $\Phi_2 = \nu_2(t_2 + t_3) + 3\pi/2$, and $\Phi_3 = (\nu_3 - \nu_1 - \nu_2)t_3 + \pi$, it can be seen that the final system state is the desired state Eq (2.48). In Fig. 5 we give evolution of four system state population in detail, where for simplify we choose $\Omega_{12} = \Omega_{24} = \Omega_{34} = \Omega$. Phase terms of coupling and interaction time between each radio frequency pulse and spin are chosen as discussed earlier.

From Fig. 5 we can see that starting from initial state $|1\rangle$ after step by step turning on three radio frequency pulses between corresponding levels, the final pop-

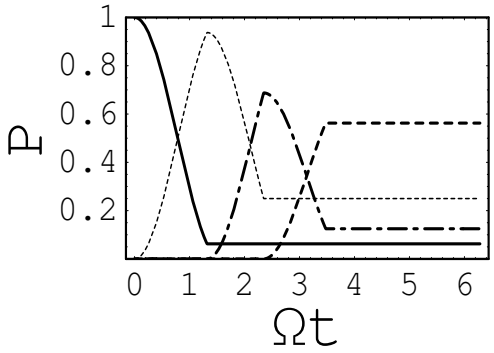

Fig. 5. Schematics for the Population dynamics of the four levels. Solid line is state $|1\rangle$, dot line is state $|2\rangle$, dash dot line line is state $|4\rangle$ and dash line is state $|3\rangle$. For convenient we choose all the coupling constant $\Omega_{12} = \Omega_{24} = \Omega_{34} = \Omega$.

ulations of four basis end up as desired. Probability of state $|1\rangle$ at $\Omega t = 0$ is 1, at $\Omega t = 1.32$ it drops to 0.06 and keep this value till the end of preparation. For state $|2\rangle$ the probability rises from 0 to 0.94 between $\Omega t = 0$ and $\Omega t = 1.32$ and drops to 0.25 at $\Omega t = 2.35$, after that time the population will not change. There is no population on state $|4\rangle$ till time $\Omega t = 1.32$, after that the probability increases to 0.69 at $\Omega t = 2.35$ and decreases to 0.13 at $\Omega t = 3.48$ and not change after this time. The last state $|3\rangle$ will appear at $\Omega t = 2.35$ and probability increases to 0.56 at $\Omega t = 3.48$ which is the end time of state preparation.

We also plots the phases change in state coefficient during the time evolution. We choose $\nu_1 = 50\Omega$, $\nu_2 = 100\Omega$ and $\nu_3 = 25\Omega$. From Fig. 6 we can see by controlling the phase of radio frequency pulses, the phase requirements in desired state are satisfied. We restrict the phase value between 0 and 2π. θ_1 will oscillate from 0 to 2π with period $T_1 = 1/\nu_1 = 1/(50\Omega)$ during preparation time(from $\Omega t = 0$ to $\Omega t = 3.48$) and end up at value $\theta_1 = \frac{\pi}{2}$ which is desired value. Similarly final value θ_2 is desired value π and θ_3 is $\frac{3\pi}{2}$. There are no value before $\Omega t = 2.35$ for θ_2 and no value for θ_3 before $\Omega t = 1.32$. The oscillation period of θ_2 is $T_2 = 1/\nu_3 = 1/(25\Omega)$ between $\Omega t = 2.35$

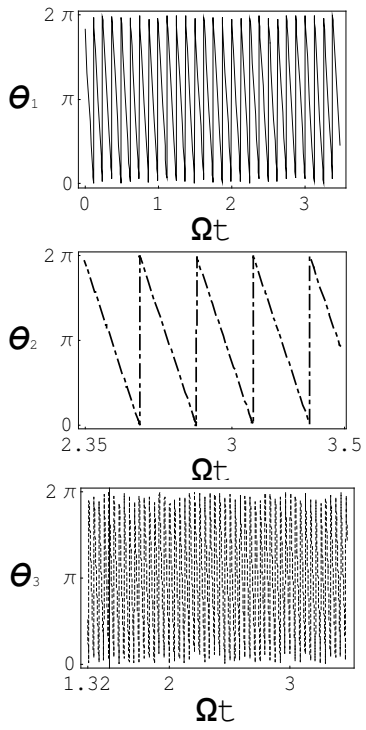

Fig. 6. Schematics for the Phase change in the coefficients of states $|2\rangle$, $|3\rangle$ and $|4\rangle$. Solid line is for θ_1, dash dot line is state for θ_2, dot line line is for θ_3. We choose $\nu_1 = 50\Omega$, $\nu_2 = 100\Omega$ and $\nu_3 = 25\Omega$

and $\Omega t = 3.48$. The oscillation period of θ_3 is $T_3 = 1/(\nu_1 + \nu_2) = 1/(150\Omega)$ between $\Omega t = 1.32$ and $\Omega t = 3.48$ which is much smaller than T_1 and T_2.

CHAPTER III

CAVITY QED BASED QUANTUM WALK

In this chapter, we present a study of the properties of quantum walks in one dimension using cavity QED method. We consider a possible experimental scheme to implement a quantum walk via an interaction between photons and a special two-level atom inside a high-Q cavity. We are interested in a random walk such that the displacement of the particle making the walk corresponds to the number of photons inside the cavity. As photon numbers are always positive, our quantum walk takes place on a straight line with an integer lattice but restricted to a half space, i.e., it can not go to negative range. The particle starts at one of those lattice points at some initial time and at each time step it moves to the left or the right lattice point with equal probability. A one-dimensional classical random walk can be described as follows. A particle starts at an initial position. The decision to move to the left or right is made by flipping a coin. If the outcome is 'heads' the particle moves to the right and if the outcome is 'tails', the particle moves to the left. It is well known that the probability of being at a given position remains maximum at the initial position. For large number of steps, the distribution is given by a Gaussian. The results for quantum walk are qualitatively different. The basic difference comes from the fact that, in a quantum walk, we consider the probability amplitudes for the displacement instead of probabilities. As a consequence there is quantum interference between the probability amplitudes at different locations. One interesting feature is that the probability for location at the initial location is no longer maximum.

In the case of the quantum walk, the particle moves to the left or right according to the outcome of the flip of a 'quantum coin' as determined by the chirality [36]. At any point of the lattice the particle has either 'left' or 'right' chirality. The chirality

undergoes a rotation (a unitary transformation called 'Hadamard transformation') according to

$$\begin{aligned} |L\rangle &\longrightarrow \frac{1}{\sqrt{2}}(|L\rangle + |R\rangle) \\ |R\rangle &\longrightarrow \frac{1}{\sqrt{2}}(|L\rangle - |R\rangle) \end{aligned} \tag{3.1}$$

The particle then moves to the adjacent lattice point according to its final chirality state, i.e.,

$$\begin{aligned} |\psi_L(n,t)\rangle &\longrightarrow |\psi_L(n-1,t)\rangle \\ |\psi_R(n,t)\rangle &\longrightarrow |\psi_R(n+1,t)\rangle \end{aligned} \tag{3.2}$$

Here $|\psi_L(n,t)\rangle$ and $|\psi_R(n,t)\rangle$ are the wave functions of the particle at position 'n' at time step 't' with 'left' or 'right' chirality. A simulation of such a quantum walk is presented in Fig. 7. We plot the probabilities $P_{L,n}$ and $P_{R,n}$ which are the probabilities with the left and right chiralities, respectively, for the particle at positions n after $t = 100$ steps. Initially the particle is located at n=0 and will move to the left.

We now introduce a cavity QED scheme for the implementation of the quantum walk discussed above. The proposed scheme is based on the interaction of an atom with an array of classical and quantum radiation fields. However, before describing our scheme, we define certain operations that can be carried out in the atom-field interaction.

(a) First we consider the resonant interaction of a two-level atom with a classical field. The unitary operator corresponding to this interaction is given by [19]

$$U_C(\theta,\varphi) = \begin{pmatrix} \cos(\theta) & -ie^{i\varphi}\sin(\theta) \\ -ie^{-i\varphi}\sin(\theta) & \cos(\theta) \end{pmatrix}, \tag{3.3}$$

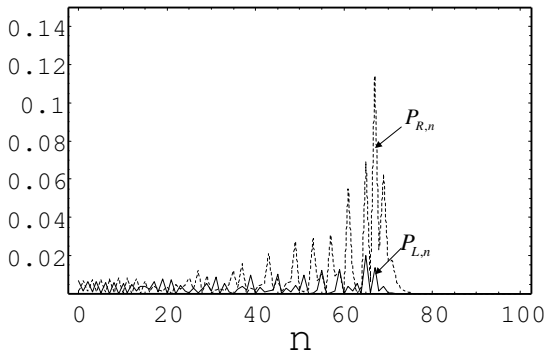

Fig. 7. The probabilities $P_{L,n}$ and $P_{R,n}$ are plotted versus n. At initial time the particle is located at the position $n_0 = 0$ and moving direction is left. Total number of steps is $t = 100$.

where $\theta = \Omega\tau$ with Ω being the Rabi frequency and τ is the interaction time, and φ is the phase of the driving field.

(b) Secondly we consider the interaction of a two-level atom with the quantized field inside cavity and we discuss how a shift of the photon number state can take place via chirping. We assume that the detuning between the atomic transition frequency ω_{ab} and the cavity resonance frequency ν is time dependent (See Fig. 8). The atom-field interaction in the dipole and the rotating-wave-approximation is described by the following Hamiltonian:

$$\begin{aligned} \mathcal{H}_0 &= \hbar\nu \left|a\right\rangle \left\langle a\right| + \hbar\nu a^\dagger a + \\ &\quad \hbar\delta(t) \left|a\right\rangle \left\langle a\right| + \hbar g(\left|a\right\rangle \left\langle b\right| a + a^\dagger \left|b\right\rangle \left\langle a\right|) \end{aligned} \tag{3.4}$$

where $\delta(t) = \omega_{ab} - \nu$ is the atom-field detuning. The Hamiltonian can be diagonalized

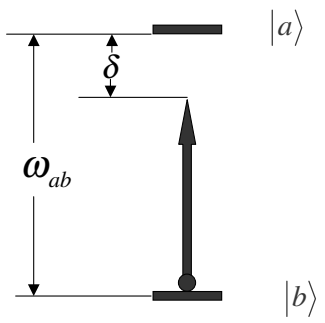

Fig. 8. Schematics of a two-level atom interacting with the radiation field. The energy levels $|a\rangle$ and $|b\rangle$ of the atom are detuned from the radiation field of frequency ν by an amount $\delta = \omega_{ab} - \nu$.

and the atom-field dressed states are given by

$$\begin{aligned} |+\rangle &= \cos\theta_n |a\rangle |n\rangle - \sin\theta_n |b\rangle |n+1\rangle \\ |-\rangle &= \sin\theta_n |a\rangle |n\rangle + \cos\theta_n |b\rangle |n+1\rangle . \end{aligned} \tag{3.5}$$

The corresponding energy eigenvalues are

$$\begin{aligned} E_{+n} &= \hbar((n+1)\nu + \omega_{ab}) - \frac{\hbar}{2}(\sqrt{\delta^2 + 4g^2(n+1)} + \delta) \\ E_{-n} &= \hbar(n\nu) + \frac{\hbar}{2}(\sqrt{\delta^2 + 4g^2(n+1)} + \delta) \end{aligned} \tag{3.6}$$

Here

$$\sin\theta_n = \frac{\sqrt{\delta^2 + 4g^2(n+1)} + \delta}{\sqrt{(\sqrt{\delta^2 + 4g^2(n+1)} + \delta)^2 + 4g^2(n+1)}},$$

$$\cos\theta_n = \frac{2g\sqrt{n+1}}{\sqrt{(\sqrt{\delta^2 + 4g^2(n+1)} + \delta)^2 + 4g^2(n+1)}}$$

We now consider the situation when the atom is initially in state $|b\rangle$ and there are n photon in the cavity. If the atom-field detuning is initially (at $t = t_i$) such that

$\delta = -|\delta|$ with $|\delta| >> 2g\sqrt{n+1}$, then we are in $|+\rangle$ state. Next the detuning is chirped slowly such that, at $t = t_f$(with $|t_i - t_f| >> 2g\sqrt{n+1}$), we have $\delta = +|\delta|$. The atom is then transferred to the $|b\rangle$ with $n+1$ photons. Thus the net result of frequency chirping is that

$$|a\rangle |n\rangle \rightarrow -|b\rangle |n+1\rangle .$$

It is not difficult to see that, under the same circumstances, the atom-field state $|b\rangle |n\rangle$ evolves to $|a\rangle |n-1\rangle$. Thus we can describe an operator S such that

$$S : |a\rangle |n\rangle \longrightarrow -|b\rangle |n+1\rangle$$

$$S : |b\rangle |n\rangle \longrightarrow |a\rangle |n-1\rangle$$

It may be noted that this transformation takes place regardless of the number of photons n inside the cavity.

Generally from Eq. 3.5 we can make evolution: $|a\rangle |n\rangle \longrightarrow (-\alpha^2+\beta^2)|b\rangle |n+1\rangle + (2\alpha\beta)|a\rangle |n\rangle$ and $|b\rangle |n+1\rangle \longrightarrow (\alpha^2 - \beta^2)|a\rangle |n\rangle + (2\alpha\beta)|b\rangle |n+1\rangle$ if detuning is changed from $\delta = -|\delta|$ at $t = t_i$ to $\delta = |\delta|$ at $t = t_f$ adiabatically, where $\alpha = \cos\theta_n|_{\delta=-|\delta|}$ and $\beta = \sin\theta_n|_{\delta=-|\delta|}$ and $|\delta|$ is the largest detuning value. The condition to use adiabatic passage approach is $T = |t_i - t_f| >> \frac{g\sqrt{n+1}}{\delta(2\omega_{ab}-3\delta)}$ if chirping process follows relation :$\delta = 2|\delta|\frac{t}{T} - |\delta|$, It can be seen that if $\frac{g}{\delta}$ is small enough then it is not necessary to wait a long interaction time T for adiabatic process to be completed. While in simulation we choose $\frac{g}{|\delta|}$=0.01 which makes evolution almost same as operation S since here $\alpha = \cos\theta_n|_{\frac{g}{\delta}=-0.01} \approx 1$ and $\beta = \sin\theta_n|_{\frac{g}{\delta}=-0.01} \approx 0$.

Now we are ready to discuss the implementation of a quantum walk based only on the operations $U_C(\theta, \varphi)$ and S.

We consider the passage of a two-level atom through a cavity. The initial state

of the atom can be the ground state $|b\rangle$ or the excited state $|a\rangle$ and the cavity is in the photon number state $|n_0\rangle$. We now show that each step of the quantum walk corresponds to a sequence of the operations $U_C(\pi/2, -\pi/2)SU_C(\pi/4, -\pi/2)$. Thus for each step, we need two interactions with the classical fields supplemented by an time-dependent interaction with the quantized cavity field.

The atomic states $|b\rangle$ and $|a\rangle$ correspond to 'left' and 'right' chirality states needed in quantum walks. The photon number states in the cavity represent particle positions. The changing of the photon number corresponds to a particle moving forward or backward. As pointed out earlier, the photon number is non-negative. Therefore our study concerns only half space in quantum walks, i.e., the particle is restricted in non-negative range.

We start the first step of quantum walk with Hadamard transformation of chirality states $|a\rangle$ and $|b\rangle$. This step can be simply carried out via interaction between classical field and the two-level atom system. The unitary classical evolution matrix is given as:

$$U_C(\pi/4, -\pi/2) = \frac{1}{\sqrt{2}} \begin{pmatrix} 1 & -1 \\ 1 & 1 \end{pmatrix} \tag{3.7}$$

The atomic states $|a\rangle$ and $|b\rangle$ evolve to

$$\begin{aligned} |a\rangle &\longrightarrow \frac{1}{\sqrt{2}}(|a\rangle + |b\rangle) \\ |b\rangle &\longrightarrow \frac{1}{\sqrt{2}}(|b\rangle - |a\rangle) \end{aligned} \tag{3.8}$$

Please note that there is a slight difference between Eq. (3.8) and Eq. (B) but it does not affect the final result of quantum walks.

In the second step, we change the photon states according to the following prescription: Photon numbers increase by one if the atom is in state $|a\rangle$ and decrease by

one if atom is in state $|b\rangle$ without changing the atom states, i.e.,

$$|b\rangle\,|n\rangle \longrightarrow |b\rangle\,|n-1\rangle$$
$$|a\rangle\,|n\rangle \longrightarrow |a\rangle\,|n+1\rangle \tag{3.9}$$

This step can not be accomplished through a simple Jaynes-Cummings type interaction. Instead we consider a two-step process. In the first step we use a frequency chirping method represented by S as discussed in (b) above. The result is $S : |a\rangle\,|n\rangle \longrightarrow -|b\rangle\,|n+1\rangle$ and S:$|b\rangle\,|n\rangle \longrightarrow |a\rangle\,|n-1\rangle$

Next we use classical evolution (Eq. (3.3)) with $\theta = \pi/2$ and $\varphi = -\pi/2$, i.e.,

$$U_C(\pi/2, -\pi/2) = \begin{pmatrix} 0 & -1 \\ 1 & 0 \end{pmatrix} \tag{3.10}$$

to make -$|b\rangle\,|n+1\rangle \longrightarrow |a\rangle\,|n+1\rangle$ and $|a\rangle\,|n-1\rangle \longrightarrow |b\rangle\,|n-1\rangle$. Thus finally we have

$$\begin{aligned} |a\rangle\,|n\rangle &\longrightarrow -|b\rangle\,|n+1\rangle \longrightarrow |a\rangle\,|n+1\rangle \\ |b\rangle\,|n\rangle &\longrightarrow |a\rangle\,|n-1\rangle \longrightarrow |b\rangle\,|n-1\rangle \quad \text{if } n > 0 \\ |b\rangle\,|0\rangle &\longrightarrow |b\rangle\,|0\rangle \longrightarrow |a\rangle\,|0\rangle \quad \text{if } n = 0. \end{aligned} \tag{3.11}$$

The operation of the first and the second steps, i.e., $U_C(\pi/2, -\pi/2)SU_C(\pi/4, -\pi/2)$ completes the description of one step of the quantum walk. Repeating these steps again and again we can make quantum walks.

The immediate question arises as to how we can control the classical evolution as well as the time-dependent evolution for chirping during the passage of atom through the cavity. We propose the atomic levels $|a\rangle$ and $|b\rangle$ to be magnetic sublevels

coupled through appropriately polarized light. The interactions can then be controlled via application of time dependent magnetic field such that the interaction times for the implementation of the $U_C(\theta, \varphi)$ transformation and the time dependence of the detuning Δ for the chirping is controlled.

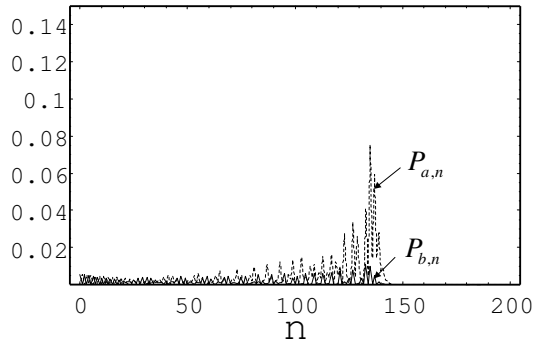

Fig. 9. The probabilities $P_{a,n}$ and $P_{b,n}$ are plotted versus n. These plots show the photon numbers after 200 time steps, the initial photon number is $n_0 = 0$.

In Fig. 9-11, we present results of our simulation. We choose initial states to be $|b\rangle\,|n_0\rangle$. For each figure, we give the value of the initial photon numbers n_0 and the total number of time steps. In these figures $P_{a,n}$ and $P_{b,n}$ represent the probabilities for the atom to be in state $|a\rangle$ and $|b\rangle$, respectively, with n photons inside the cavity.

In Fig. 9 we choose n_0=0 and time step=200. The quantum walks in our system can not go to negative range ($n \geq 0$). The maximum probability of photon states therefore lies in the range $n = 0$ to $n = 200$. For a larger number of quantum steps, the maximum probability of photon states moves away from $n = 0$ as shown in Fig. 3.

In Fig. 10 we chose n_0=100 and the number of time steps to be equal to 100 as well. The quantum walks can now take place on both sides of $n = 100$. The shape

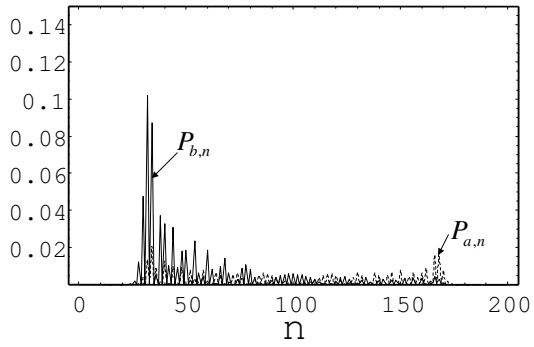

Fig. 10. The probabilities $P_{a,n}$ and $P_{b,n}$ are plotted versus n. Here we set the initial photon number n_0=100, and the number of steps are 100.

of the probability is not symmetrical and is dependent on the initial atomic state. This is one of the important differences between classical random walk and quantum walk. The maximum probability of photon states lies on the left side of $n = 100$ for the initial state $|b\rangle$.

In Fig. 11, we consider the case of $n_0 = 100$ and the number of time steps t=200. Quantum walk with one barrier has been studied By Bach et al.[39]. Here the wave will move from $n_0 = 100$ to the right and left as Fig. 4, but this time the left going wave will reach $n = 0$ and then bounce back to $n > 0$. An interference between the left going and right going walks leads a complex behavior between $n = 0$ to $n = 100$.

Since at present it is impossible to have pure photon number state for large photon number, in Fig. 11, we choose initial photon states to be coherent state and give final result of quantum walk.

For initial field state as coherent stateα, $|\alpha\rangle = e^{-|\alpha|^2/2} \sum_n^\infty \frac{\alpha^n}{\sqrt{n!}} |n\rangle$ where α is a complex number and $|\alpha|^2 = \langle n\rangle$ is average photon number, in Fig. 12 we choose average photon number=100. We make quantum walk as before for different Fock

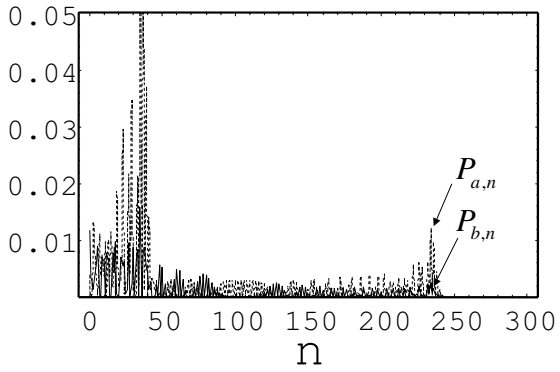

Fig. 11. The probabilities $P_{a,n}$ and $P_{b,n}$ are plotted versus n. Here initial photon number is n_0=100 and total number of time steps are 200.

state separately and combine their distribution together to get final result of photon distribution for different atom levels in quantum walk. Comparing with Fig.4 we can see the sharp peak and dip will disappear because initial state is a mixed state in Fock space and there are also distribution of odd photon number state as Fig.11, the reason is there are distributions of odd photon state in initial field this time.

Since classical characters of coherent states are so obvious then it is possible to do experiment to test this kind of coherent state quantum walk.

Decoherence induced by losses through the cavity mirrors will affect our quantum walk because the photon number inside the cavity will change as time goes on, so in our study it is assumed that mirror is lossless.

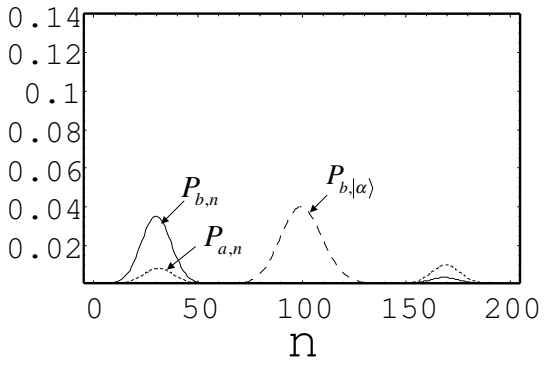

Fig. 12. Diagram of P_{an} and P_{bn} verse n, here we set initial photon number as coherent state $|\alpha\rangle$ and $|\alpha|^2 = \langle n\rangle = 100$, and give the probability distributions in state $|a\rangle$ or in state $|b\rangle$ for different photon numbers after time step t=100

CHAPTER IV

PROPERTIES OF CLASSICAL AND QUANTUM TELEPORTATION

A. Quantum teleportation of an arbitrary superposition of atomic Dicke states

First we introduce quantum teleportation of an arbitrary superposition of atomic Dicke states. we consider a departure from the usual teleportation scenario in two ways. First, following an interesting recent suggestion [80], the entanglement resource necessary for teleportation is not introduced as shared particles between Alice and Bob, but rather comes about from a detection made by Alice of the joint state of both parties following independent preparation stages. Second, and central to the present paper, the state that is to be teleported is itself an arbitrary entangled state of many particles, constituting the most general transfer of quantum information between the two parties.

However, we note that photons have an intrinsic advantage in that they are better suited for communication over long distances. Cavity QED methods offer an ideal coupling between atoms and photons in a controlled setting [19]. Based on such methods, we can achieve quantum teleportation of entangled states in multiple cavities, as well as arbitrary superpositions of Fock states in a single cavity.

In the present proposal, we take a different approach to scalable quantum teleportation. Some past studies have used the joint detection of photon decays to establish entanglement among distant atoms [81, 82]. In a novel application of this idea, Bose *et al.* [80] show how to teleport an atomic state from one cavity to another by conditional detection of a photon from both cavities. The main advantage of their scheme is the use of photon decays themselves to establish entanglement between the cavities, rather than the cumbersome task of coherently coupling a photon out of one cavity

and feeding it into another cavity [83, 84].

We consider the use of multi-atom dark states for quantum state transfer and teleportation, where the desired inter-cavity entanglement is

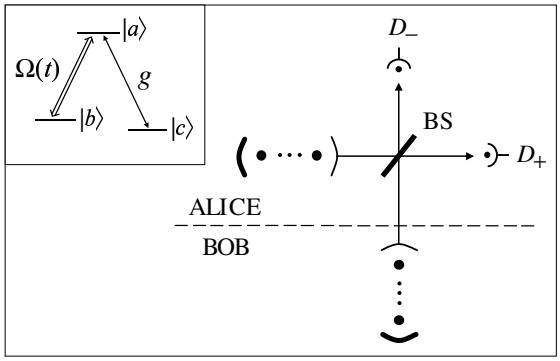

Fig. 13. Setup for teleporting an arbitrary superposition of atomic Dicke states. Inset shows the level configuration of each atom.

brought about by a sequence of conditional detections of photons leaking out of both cavities. The main advantage of the proposed scheme is the ability to transfer multi-qubit entangled states, namely superpositions of atomic Dicke states [85], which can be engineered in a cavity by conditional detection methods, and have wide ranging applications in quantum information science (see [86]).

Our scheme is shown in Fig. 13. Alice and Bob have an equal number of (identical) atoms trapped inside their cavities, and the atoms are well separated so that any interaction between them can be neglected. The cavities are designed to be one sided so that the direction of cavity leakage is known, and photons leaking out of the cavities pass through a beam splitter BS and are detected by two 100 percent efficient detectors D_+ and D_-, which we treat using the quantum jump formalism [19, 87].

In section 1, we discuss the two-atom case first, as it allows us to highlight the key physics that goes into making each stage possible. We highlight the different control

parameters that are unique to this protocol, and also briefly describe methods for unitary post-processing of the teleported state to optimize the fidelity. In section 2, we show that the protocol can be generalized to an arbitrary number of atoms, and discuss the scaling of the success probability with the number of atoms. In section 3, we discuss issues related to fidelity optimization and experimental feasibility of the protocol, and extensions to other quantum information applications.

1. Two-atom teleportation

The atomic state in cavity A which Alice wants to teleport is assumed to be a (symmetric) Dicke-state superposition of the form

$$|\psi\rangle_A^{\text{in}} = C_0^I |cc\rangle_A + C_1^I \frac{|bc\rangle_A + |cb\rangle_A}{\sqrt{2}} + C_2^I |bb\rangle_A , \tag{4.1}$$

where $|a\rangle$, $|b\rangle$ and $|c\rangle$ are the states of each Λ-type three-level atom (see Figure 1 inset). States $|cc\rangle$ and $|bb\rangle$ represent both atoms in the same state, and $(|bc\rangle + |cb\rangle)/\sqrt{2}$ is a state with one atom in state $|b\rangle$ and one in state $|c\rangle$. The coefficients C_0^I, C_1^I, and C_2^I are arbitrary and satisfy $\left|C_0^I\right|^2 + \left|C_1^I\right|^2 + \left|C_2^I\right|^2 = 1$.

Our protocol is based on a mapping of the two-atom state in Eq. (4.1) to an equivalent Fock state superposition of the cavity field consisting of 0, 1, or 2 photons. This is done using multi-atom dressed state adiabatic passage in the cavity in the presence of a classical drive field, which has the ability to generate atom-field entanglement. However, we have to be careful because while the adiabatic passage is taking place, the photons can leak out and be detected. Conditional detection of photons is necessary for our scheme because it leads to 'quantum jumps' that enables the Dicke state transfer. Thus, before proceeding, we examine the quantum jump formalism and how it applies in the multi-atom dark state picture.

In each cavity, the atoms are assumed to be simultaneously coupled to a time-

dependent classical field, with Rabi frequency $\Omega(t)$, and a quantized cavity field mode with coupling strength g. The interaction is governed by the Hamiltonian [19]

$$\begin{aligned} H &= \hbar\Omega(t)(|a_1\rangle\langle b_1| + |b_1\rangle\langle a_1|) \\ &\quad +\hbar g(|a_1\rangle\langle c_1|\,\hat{a} + |c_1\rangle\langle a_1|\,\hat{a}^\dagger) + (1 \to 2), \end{aligned} \tag{4.2}$$

where 1 and 2 enumerate the atoms, and $\hat{a}^\dagger$ and $\hat{a}$ are photon creation and destruction operators. Now, conditional on the *absence* of a click in the detectors, the effective Hamiltonian governing the time evolution of the joint state is given by [88, 89]

$$H_{\text{eff}} = H - i\kappa\hat{a}^\dagger\hat{a}. \tag{4.3}$$

Here, κ is the decay rate of the field mode $\hat{a}$, taken to be the same for both cavities. Note that H_{eff} is non-Hermitian due to the presence of the decay term. However, we can still define an effective 'interaction picture' where the atom-field evolution is described by the Hamiltonian

$$H_I = \exp(\kappa\hat{a}^\dagger\hat{a}t)\, H \exp(-\kappa\hat{a}^\dagger\hat{a}t), \tag{4.4}$$

and the corresponding state vector

$$|\Psi_I\rangle = \exp(\kappa\hat{a}^\dagger\hat{a}t)|\Psi\rangle. \tag{4.5}$$

In this way, by switching between pictures, we can treat the atom-field coupling separately from the decay of the field from the cavity. By numerically solving Schrödinger's equation, we have verified that H_{eff} and H_I describe identical evolutions of the state in the respective pictures.

Finally, when detection events do occur, the quantum jump formalism associates these with the action of photon annihilation operators. For the two detectors $D_\pm$ in

our scheme (Figure 1), we have the linear transformations due to the beam splitter:

$$\hat{D}_+ = (t\hat{a}_A + r\hat{a}_B); \tag{4.6}$$

$$\hat{D}_- = (r\hat{a}_A - t\hat{a}_B), \tag{4.7}$$

where $\hat{a}_A$ ($\hat{a}_B$) is the destruction operator for the field in cavity A (B), and r and t are the (real) reflection and transmission coefficients for the beam splitter, such that $|r|^2 + |t|^2 = 1$.

A key to our approach is the use of multi-atom dark states in each cavity (see, for example, Ref. [90]). It is convenient to classify the states according to the total number of excitations present. For zero excitation, we have both atoms in state $|c\rangle$ and field in vacuum:

$$|\Psi_0^{\rm dark}\rangle = |cc\rangle|0\rangle. \tag{4.8}$$

For one excitation, the manifold of states coupled by the Hamiltonian H (i.e. having non-zero matrix elements) are $|cc\rangle|1\rangle$, $|bc\rangle|0\rangle$, $|cb\rangle|0\rangle$, $|ac\rangle|0\rangle$, and $|ca\rangle|0\rangle$. From these, we can construct two states that are dark with respect to the couplings Ω and g for each atom (i.e. zero-eigenvalue states of H):

$$|\Psi_1^{\rm dark}\rangle_j \propto |b_j\rangle|0\rangle - (\Omega/g)|c_j\rangle|1\rangle, \tag{4.9}$$

for $j = 1$ or 2. The effects of cavity decay may be included in the interaction picture (defined by H_I) by replacing g with $ge^{-\kappa t}$. For two excitations, the manifold of coupled states consists of $|cc\rangle|2\rangle$, $|bc\rangle|1\rangle$, $|cb\rangle|1\rangle$, $|bb\rangle|0\rangle$, $|ba\rangle|0\rangle$, $|ab\rangle|0\rangle$, and $|aa\rangle|0\rangle$, which supports a two-atom dark state:

$$\begin{aligned} |\Psi_2^{\rm dark}\rangle \propto\ & |bb\rangle|0\rangle - [\sqrt{2}(\Omega/g)](|bc\rangle + |cb\rangle)|1\rangle/\sqrt{2} \\ & + [(\Omega/g)^2/\sqrt{2}]|cc\rangle|2\rangle. \end{aligned} \tag{4.10}$$

In the preparation stage, Alice follows the above dark states, and by tuning $\Omega(t)$ to go from $\Omega \ll g$ to $\Omega \gg g$, achieves the following adiabatic transformations:

$$|cc\rangle_A|0\rangle_A \rightarrow |cc\rangle_A|0\rangle_A, \tag{4.11}$$

$$|bc\rangle_A|0\rangle_A \rightarrow |cc\rangle_A|1\rangle_A, \tag{4.12}$$

$$|cb\rangle_A|0\rangle_A \rightarrow |cc\rangle_A|1\rangle_A, \tag{4.13}$$

$$|bb\rangle_A|0\rangle_A \rightarrow |cc\rangle_A|2\rangle_A, \tag{4.14}$$

where in the last line, we have used the approximation that $(\Omega/g)^2 \gg 2(\Omega/g)$ since $\Omega \gg g$. In this way, she transfers her given atomic state in Eq. (4.1) to the corresponding field state in time t_p, resulting in the atom-field state

$$|\Psi\rangle_A = \left(C_0\,|0\rangle_A + C_1\,|1\rangle_A + C_2\,|2\rangle_A\right)|cc\rangle_A/\sqrt{N_1}, \tag{4.15}$$

where, including the effects of cavity decay, we have

$$C_0 = C_0^I, \tag{4.16}$$

$$C_1 = e^{-\kappa t_p}\sqrt{2}C_1^I, \tag{4.17}$$

$$C_2 = e^{-2\kappa t_p}C_2^I, \tag{4.18}$$

and $N_1 = |C_0|^2 + |C_1|^2 + |C_2|^2$ is for normalization.

At the same time, Bob places two atoms in his cavity B in the state $|b\rangle$, and by tuning $\Omega(t)$, evolves his system from $|bb\rangle_B|0\rangle_B$ to the two-atom dark state $|\Psi_2^{\rm dark}\rangle$ at time $t = t_p$:

$$\begin{aligned} |\Psi\rangle_B = &\left(D_0|bb\rangle_B|0\rangle_B + D_1\frac{|bc\rangle_B + |cb\rangle_B}{\sqrt{2}}\,|1\rangle_B\right. \\ &\left. + D_2|cc\rangle_B|2\rangle_B\right)/\sqrt{N_2}, \end{aligned} \tag{4.19}$$

where $D_0 = 1$, $D_1 = -\sqrt{2}(\Omega/g)$, $D_2 = (\Omega/g)^2/\sqrt{2}$, and $N_2 = |D_0|^2 + |D_1|^2 + |D_2|^2$. Note that cavity decay does not affect the relative amplitudes of the dark state, as this is always defined with respect to the original Hamiltonian H. However, and this is the key trick, Bob can choose $\Omega(t_p)/g$ to be of the form $\alpha e^{-\kappa t_p}$ to complement the decay in Alice's cavity:

$$D_0 = 1, \tag{4.20}$$

$$D_1 = -\alpha\sqrt{2}e^{-\kappa t_p}, \tag{4.21}$$

$$D_2 = (\alpha^2/\sqrt{2})e^{-2\kappa t_p}. \tag{4.22}$$

To summarize, following independent preparations, the joint state of Alice's and Bob's systems is

$$|\Psi\rangle_{AB}^{\text{in}} = |\Psi\rangle_A \otimes |\Psi\rangle_B. \tag{4.23}$$

In the detection stage, Alice waits for two (and only two) clicks on her detectors from photons arriving from both cavities. The first click occurs at time $t = t_1$ after preparation, and the second click occurs at time $t = t_2$ after preparation. The simultaneous detection process leaves the joint state of Alice and Bob in (see Appendix)

$$\begin{aligned} |\Psi\rangle_{AB}^{\text{out}} &\propto \hat{D}^{\pm} e^{-\kappa \hat{a}^\dagger \hat{a}(t_2 - t_1)} \hat{D}^{\pm} e^{-\kappa \hat{a}^\dagger \hat{a} t_1} |\Psi\rangle_A \otimes |\Psi\rangle_B \\ &\propto |\psi\rangle_B^{\text{out}} |cc\rangle_A |0\rangle_A |0\rangle_B + e^{-\kappa t_2} [\cdots], \end{aligned} \tag{4.24}$$

where the cumulative time decay $e^{-\kappa t_2}$ damps out the non-zero, final photon number contributions (denoted by the dots), and we are left in the long-time regime with the following decoherence-free atomic state in Bob's cavity:

$$\begin{aligned} |\psi\rangle_B^{\text{out}} = &\left(\eta_0 C_0^I |cc\rangle_B + \eta_1 C_1^I \frac{|bc\rangle_B + |cb\rangle_B}{\sqrt{2}}\right. \\ &\left. + \eta_2 C_2^I |bb\rangle_B \right)/\sqrt{N_3}, \end{aligned} \tag{4.25}$$

where $N_3 = \left|\eta_0 C_0^I\right|^2 + \left|\eta_1 C_1^I\right|^2 + \left|\eta_2 C_2^I\right|^2$, and the coefficients η_m are given in Figure 14 for the three detection scenarios. To complete the teleportation protocol, Alice needs to inform Bob (by classical means) which detectors clicked, and Bob performs unitary operations to his final state (see below) to make his final teleported state $|\psi\rangle_B^{\text{out}}$ look as close as possible to the initial state $|\psi\rangle_A^{\text{in}}$.

	η_0	η_1	η_2
D_+D_+	$(\alpha^2/\sqrt{2})r^2$	$-(2\sqrt{2}\,\alpha)rt$	t^2
D_-D_-	$(\alpha^2/\sqrt{2})t^2$	$(2\sqrt{2}\,\alpha)rt$	r^2
D_+D_-	$-\alpha^2 rt$	$2\alpha(t^2-r^2)$	$\sqrt{2}\,rt$

Fig. 14. Pre-factors for the different detection scenarios in the final teleported state $|\psi\rangle_B^{\text{out}}$ for two atoms. r and t are the reflection and transmission coefficients for the beam splitter, and $\alpha = (\Omega/(ge^{-\kappa t_p})$ is the dark state parameter that Bob chooses initially.

The raw fidelity of the protocol, $F = |\langle\psi_{\text{in}}|\psi_{\text{out}}\rangle|^2$, depends on both the state to be teleported (the coefficients C_m^I) and the detection scenario that is realized. If only one of the Dicke states is present initially ($C_m^I = 1$ for some m), then the fidelity is automatically unity when the protocol succeeds (i.e. when two and only two clicks are recorded). For the entire superposition, the fidelity depends on the *post-processing* of the teleported state. That is, knowing the coefficients η_m in Figure 14 allows us to choose an appropriate unitary transform (that depends on the detection scenario) to maximize the fidelity after the protocol has ended. We emphasize that this *does not* depend on the initial choice of α and r, as any detection scenario can be optimized post-detection by subsequent unitary evolution of the teleported state $|\psi\rangle_B^{\text{out}}$. The free parameters α and r are chosen only to ensure that all the pre-factors η_m are non-zero.

Thus, the probability of success of the teleportation protocol depends solely on

the fact that we get two, and only two, clicks on both detectors. Note that the possibilities include [cf. Eqs. (4.15), (4.19), and (4.23)] zero, one, or two photons from each cavity, leading to 0-4 clicks in both detectors. We analyze the success probability in more detail below.

2. N_a-atom teleportation

To appreciate the scaling of the protocol, we discuss the generalization of our scheme to an arbitrary number of atoms N_a in each cavity. The interaction Hamiltonian in Eq. (4.2) generalizes to

$$\begin{aligned} H &= \sum_{i=1}^{N_a} \big[\hbar\Omega(t)(|a_i\rangle\langle b_i| + |b_i\rangle\langle a_i|) \\ &\quad +\hbar g(|a_i\rangle\langle c_i|\,\hat{a} + |c_i\rangle\langle a_i|\,\hat{a}^\dagger\big]. \end{aligned} \tag{4.26}$$

We use the notation $|b^{\otimes m}c^{\otimes N_a-m}\rangle$ to denote a normalized, symmetric Dicke state where m atoms are in the level b and N_a-m atoms are in the level c [91]. From combinatorics, there are $P(N_a,m) = N_a!/[(N_a-m)!m!]$ terms constituting the entangled state $|b^{\otimes m}c^{\otimes N_a-m}\rangle$. The initial state to be teleported is assumed to be of the form

$$|\psi\rangle_A^{\rm in} = \sum_{m=0}^{N_a} C_m^I |b^{\otimes m}c^{\otimes N_a-m}\rangle_A. \tag{4.27}$$

Using adiabatic evolution in the presence of cavity decay, and utilizing dark states composed of an arbitrary number of atoms in the cavity [cf. see Eq. (4.29) below], Alice maps the unknown N_a-atom state given above to the equivalent photon state in time t_p:

$$|\Psi\rangle_A = \frac{1}{\sqrt{\mathcal{N}_1}}\left(\sum_{p=0}^{N_a} C_p|p\rangle_A\right)|c^{\otimes N_a}\rangle_A, \tag{4.28}$$

where $C_p = e^{-p\kappa t_p}\sqrt{P(N_a,p)}\,C_p^I$. Meanwhile, Bob prepares his cavity in the N_a-atom dark state

$$|\Psi\rangle_B \;=\; \frac{1}{\sqrt{\mathcal{N}_2}}\sum_{p=0}^{N_a} D_p |b^{\otimes N_a-p}c^{\otimes p}\rangle_B |p\rangle_B, \tag{4.29}$$

where $D_p = e^{-p\kappa t_p}(-\alpha)^p\sqrt{P(N_a,p)/p!}$, and we have used the same index p to denote complementary atomic and photonic excitations in the dark state.

In the detection stage, Alice waits for N_a clicks in the two detectors. Assuming n clicks occur in D_+ and $N_a - n$ clicks in D_-, the teleported state becomes

$$|\psi^{(n)}\rangle_B^{\text{out}} = \frac{1}{\sqrt{\mathcal{N}_3}}\sum_{m=0}^{N_a}\eta_m^{(n)} C_m^I |b^{\otimes m}c^{\otimes N_a-m}\rangle_B, \tag{4.30}$$

where for detection scenario n, the pre-factor for C_m^I is given by

$$\begin{aligned}\eta_m^{(n)} \;=\; & \sum_{i=0}^{\min(m,n)} (-1)^{n-i}\alpha^{N_a-m}\sqrt{m!}\,P(N_a,m)P(n,i) \\ & \times P(N_a-n,m-i)\,r^{n+m-2i}t^{N_a-n-m+2i}.\end{aligned}$$

Successful teleportation of the superposition state occurs when there are exactly N_a photodetection events (for N_a atoms). Assuming no clicks occur during the preparation stage ($\kappa t_p << 1$), this occurs with probability $P_{\text{suc}} = \left(\sum_m |C_m D_{N_a-m}|^2\right)/\mathcal{N}_1\mathcal{N}_2$, or

$$P_{\text{suc}}(N_a) = \frac{\sum_{m=0}^{N_a}[P(N_a,m)]^2\alpha^{N_a-m}/(N_a-m)!}{2^{N_a}\sum_{m=0}^{N_a}P(N_a,m)\alpha^{N_a-m}/(N_a-m)!} \tag{4.31}$$

A plot of this quantity is shown in Figure 15, which shows that the fall off with N_a is an inverse power law. This indicates that in principle, the success probability has a polynomial scaling with the number of atoms.

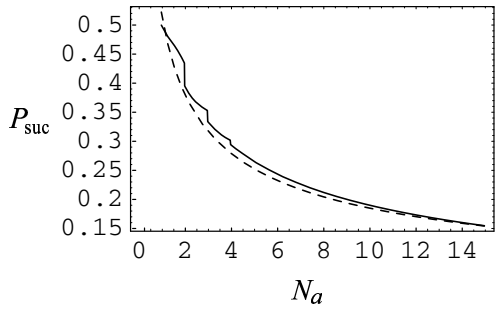

Fig. 15. The success probability of getting N_a photodetection events as a function of the number of atoms (solid line), fitted by the functional form $C/{N_a}^{0.45}$ (dashed line) for some constant C. Unit detection efficiency is assumed.

3. Discussion

First, some remarks about fidelity. We note that optimizing the fidelity after the protocol has ended defines a new problem that, to our knowledge, has not been addressed before in the teleportation literature, namely one where the weighting pre-factors $\eta_m^{(n)}$ are known, but the coefficients C_m^I of the initial state are unknown. That is, the *relative* weights of the Dicke state superposition need to be equalized regardless of their absolute amplitudes, a problem which can be posed only in a state-averaged sense. We are currently addressing this issue. To give an example, consider the two-atom case in our scheme where the final state is given by Eq. (4.25). By appropriate choice of α and r, we can arrange the pre-factors to be such that $\eta_0 < \eta_1 < \eta_2$ for all detection scenarios. To equalize these weights, we might try a two-qubit rotation of states $|bb\rangle$ and $|cc\rangle$, which leaves the symmetric state $(|bc\rangle + |cb\rangle)/\sqrt{2}$ unchanged. The optimal rotation angle is determined by averaging the fidelity over all input coefficients C_m^I. For this example, we find that the state-averaged fidelity for the two-atom case can be increased to at least 0.96 for all detection scenarios. Successive unitary operations, which will introduce more control parameters, will

further optimize this figure. A similar approach can be taken for larger number of atoms N_a, where with more atoms, we have a larger permutation of unitary operations at our disposal. Thus, the N_a-scaling is not expected to constrain the optimization.

From the experimental standpoint, the fidelity will be degraded whenever the relative amplitudes/phases of the different Dicke states are unknown, for example, due to fluctuations in laser intensity, or asymmetry in the cavity coupling to different atoms.

We believe that the technology for implementing the proposed scheme is within reach of the current state-of-the-art for a small but significant number of atoms. For example, laser cooling and trapping of individual atoms in a high-Q cavity has recently become possible [92], and optical dipole traps have been demonstrated for a deterministic number of atoms [93]. Furthermore, three-level adiabatic passage and linear optics methods are well established experimentally. The principal constraint on asymptotic scalability will be the efficiency of the detectors, which in practice will cause the success probability to decrease exponentially. Another constraint is the need for a photon number resolving detector, as we require the post-selection of the experiment based on N_a photodetection events. These issues are generic to quantum information schemes based on linear optics, and are currently active areas of research.

B. Preservation of nonclassicality in the continuous-variable quantum teleportation

Then we discuss the preservation of nonclassicality in the continuous-variable quantum teleportation. The question we address here is: Under what conditions on the squeeze parameter r and the homodyne detection efficiency η, a nonclassical input state would necessarily lose its nonclassical nature during the process of teleportation.

In this section, we first reformulate the protocol of quantum teleportation of

continuous variables of an optical field in the density matirx form and establish the relation between the P-functions of the input and output states. We then present a condition involving r and η under which the P-function of the teleported state is positive over the entire complex plane regardless of how nonclassical the input state is.

In the protocol of quantum teleportation of continuous variables, the two-mode squeezed state

$$\hat{\rho}_{ab} = \cosh^{-2}(r) e^{-\tanh(r)\hat{a}^\dagger \hat{b}^\dagger} |0\rangle \langle 0| e^{-\tanh(r)\hat{a}\hat{b}} \tag{4.32}$$

is employed as the quantum channel. In Eq. (1), r is the squeezing parameter, $\hat{a}(\hat{a}^\dagger)$ and $\hat{b}(\hat{b}^\dagger)$ are the annihilation (creation) operators for mode a which is sent to Alice and mode b which is sent to Bob, respectively. In the representation of coherent states, the input teleported state may be written as

$$\hat{\rho}_i = \int d^2\alpha P_i(\alpha) e^{-|\alpha|^2} e^{\alpha \hat{a}_i^\dagger} |0\rangle \langle 0| e^{\alpha^* \hat{a}_i}, \tag{4.33}$$

where $\hat{a}_i(\hat{a}_i^\dagger)$ is the annihilation (creation) operator for the mode to be teleported and $P_i(\alpha)$ is the P-representation of the input state.

Before teleportation, the density matrix of the entire system is

$$\hat{\rho}_t = \hat{\rho}_{ab} \otimes \hat{\rho}_i. \tag{4.34}$$

The protocol of teleportation of continuous variables is depicted in Figure 16. In the first step, Alice uses a 50:50 ideal beam splitter to couple the input mode with the entangled mode a. The beam splitter induces the unitary transformation

$$\hat{c}_1 = \frac{1}{\sqrt{2}}(\hat{a} + \hat{a}_i), \tag{4.35}$$

$$\hat{c}_2 = \frac{1}{\sqrt{2}}(\hat{a} - \hat{a}_i), \tag{4.36}$$

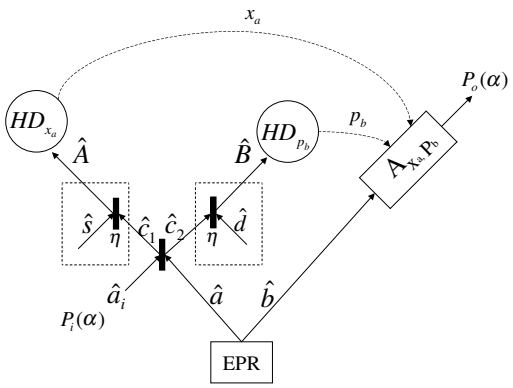

Fig. 16. Scheme for the quantum teleportation of continuous variables. Here HD_{x_a} and HD_{P_b} are homodyne detectors for measuring x_a and p_b and A_{x_a,p_b} is the amplitude displacement device. The dashed blocks represent the fictitious beam splitters with efficiency η

where $\hat{c}_1$ and $\hat{c}_2$ are the annihilation operators for two modes out of two ports of the beam splitter. In terms of annihilation and creation operators for the modes out of the beam splitter, the density matrix (3) can be rewritten as

$$\begin{aligned}\hat{\rho}_t &= \cosh^{-2}(r)\int d^2\alpha P(\alpha)e^{-|\alpha|^2} \\ &\quad e^{\frac{1}{\sqrt{2}}[\alpha(\hat{c}_1^\dagger-\hat{c}_2^\dagger)-\tanh(r)\hat{b}^\dagger(\hat{c}_1^\dagger+\hat{c}_2^\dagger)]} \\ &\quad |0\rangle\langle 0|\, e^{\frac{1}{\sqrt{2}}[\alpha^*(\hat{c}_1-\hat{c}_2)-\tanh(r)\hat{b}(\hat{c}_1+\hat{c}_2)]}. \end{aligned} \tag{4.37}$$

In the next step, two homodyne detectors are employed to measure the real part of the complex amplitude of the mode c_1 and the imaginary part of the complex amplitude of the mode c_2. Here, we assume that the detectors are nonideal and have the same amplitude efficiency $\sqrt{\eta}$. To incorporate the diminishing effects of nonideal photodetection on the amplitudes of the fields into the above formula, we replace the

bosonic annihilation operatros for the modes c_1 and c_2 by the operators

$$\hat{A} = \sqrt{\eta}\hat{c}_1 + \sqrt{1-\eta}\hat{s}, \tag{4.38}$$

$$\hat{B} = \sqrt{\eta}\hat{c}_2 + \sqrt{1-\eta}\hat{d}. \tag{4.39}$$

In order to keep $\hat{A}(\hat{B})$ and $\hat{A}^\dagger(\hat{B}^\dagger)$ having the correct commutation relations for the bosonic annihilation and creation operators, two vacuum modes described by annihilation operators $\hat{s}$ and $\hat{d}$ are introduced [94, 95]. The transformations (7) and (8) can be modeled by two fictitious beam splitters before the homodyne detectors, as shown in the dashed bolcks of Figure 16. Upon the replacement,we have

$$\begin{aligned}
\hat{\rho}_t &= \cosh^{-2}(r)\int d^2\alpha P(\alpha)e^{-|\alpha|^2} \\
&\quad e^{\sqrt{\frac{\eta}{2}}[\alpha(\hat{c}_1^\dagger - \hat{c}_2^\dagger) - \tanh(r)\hat{b}^\dagger(\hat{c}_1^\dagger + \hat{c}_2^\dagger)]} \\
&\quad Tr_v\{e^{\sqrt{\frac{1-\eta}{2}}[\alpha(\hat{s}^\dagger - \hat{d}^\dagger) - \tanh(r)\hat{b}^\dagger(\hat{s}^\dagger + \hat{d}^\dagger)]} \\
&\quad |0\rangle\langle 0|\, e^{\sqrt{\frac{1-\eta}{2}}[\alpha^*(\hat{s} - \hat{d}) - \tanh(r)\hat{b}(\hat{s} + \hat{d})]}\} \\
&\quad e^{\sqrt{\frac{\eta}{2}}[\alpha^*(\hat{c}_1 - \hat{c}_2) - \tanh(r)\hat{b}(\hat{c}_1 + \hat{c}_2)]},
\end{aligned} \tag{4.40}$$

where Tr_v represents the trace over the vacuum modes. We complete the trace calculation in the representation spanned by common eigenstates of the phase quadratue operators $\hat{x}_s = (\hat{s} + \hat{s}^\dagger)/2$ and $\hat{p}_d = (\hat{d} - \hat{d}^\dagger)/2i$ for the vacuum modes. The resulting expresion of the field density operator is

$$\begin{aligned}
\hat{\rho}_t &= \mathcal{N}\int d^2\alpha P(\alpha)e^{-\eta|\alpha|^2} \\
&\quad e^{\sqrt{\frac{\eta}{2}}[\alpha(\hat{c}_1^\dagger - \hat{c_2}^\dagger) - \tanh(r)\hat{b}^\dagger(\hat{c}_1^\dagger + \hat{c}_2^\dagger)]} \\
&\quad \hat{\rho}_{th} e^{\sqrt{\frac{\eta}{2}}[\alpha^*(\hat{c}_1 - \hat{c_2}) - \tanh(r)\hat{b}(\hat{c}_1 + \hat{c}_2)]},
\end{aligned} \tag{4.41}$$

where

$$\hat{\rho}_{th} = \sum_{n=0}^{\infty} \frac{\langle n\rangle^n}{(1+\langle n\rangle)^{n+1}} |n\rangle\langle n|, \tag{4.42}$$

$$\langle n\rangle = \frac{1-\eta\tanh^2(r)}{1-(1-\eta)\tanh^2(r)}, \tag{4.43}$$

$$\mathcal{N} = \frac{\cosh^{-2}(r)}{1-(1-\eta)\tanh^2(r)}. \tag{4.44}$$

We see that the non-unity efficiency of the homodyne detection corresponds to the excitation of modes c_1 and c_2 from the thermal state instead of vacuum.

Alice now performs a measurement on the eigenvalues of the phase quadrature operators $\hat{x}_a = (\hat{c}_1 + \hat{c}_1^\dagger)/2$ and $\hat{p}_b = (\hat{c}_2 - \hat{c}_2^\dagger)/2i$ by use of the ideal homodyne detectors. Once Alice obtained the result (x_a, p_b), the density matrix for the mode b on the Bob's side reduces to

$$\begin{aligned}\hat{\rho}(x_a,p_b) = {} & (\frac{\pi}{2})^{-1}\mathcal{N}\int d^2\alpha P(\alpha) e^{-\eta|\alpha|^2} \\ & e^{-2(x_a^2+p_b^2)+\sqrt{2\eta}[\alpha(x_a+ip_b)+c.c)]} \\ & e^{\sqrt{\eta}[\sqrt{\eta}\alpha-\sqrt{2}(x_a-ip_b)]\tanh(r)\hat{b}^\dagger} \\ & \hat{\rho}_{th} e^{\sqrt{\eta}[\sqrt{\eta}\alpha^*-\sqrt{2}(x_a+ip_b)]\tanh(r)\hat{b}}\end{aligned} \tag{4.45}$$

becuase of the quantum entanglement between the modes a and b. Alice then sends Bob the measurement result through classical channels.

According to the measurement result, Bob performs the displacement transformation $D(\Delta)$ with $\Delta = -\beta\sqrt{2}(x_a - ip_b)$ on the mode b. Here β is a parameter to be determined. In general, the parameter β should be properly chosen so that the teleportation has the maximal fidelity.

The density matrix (14) is unnormalized. The measurement probability $p(x_a, p_b)$ for the result (x_a, p_b) is $tr[\hat{\rho}(x_a, p_b)]$. On the average over the measurement results,

the normanized density matrix for the mode b is given by

$$\begin{aligned}\hat{\rho}_b &= \int dx_a dp_b D^\dagger(\Delta)\hat{\rho}(x_a,p_b)D(\Delta)\\ &= (\frac{\pi}{2})^{-1}\mathcal{N}\int d^2\alpha P(\alpha)\\ &\quad \int dx_a dp_a e^{-[1-(1+\langle n\rangle)\eta\tanh^2(r)]\left|\sqrt{\eta}\alpha-\sqrt{2}(x_a-ip_b)\right|^2}\\ &\quad \frac{1}{\pi\langle n\rangle}\int d^2\xi e^{-\frac{1}{\langle n\rangle}\left|\xi-\sqrt{\eta}\langle n\rangle tanh(r)[\sqrt{\eta}\alpha-\sqrt{2}(x_a-ip_b)]\right|^2}\\ &\quad D(X)\left|0\right\rangle\left\langle 0\right| D^\dagger(X),\end{aligned} \tag{4.46}$$

where $X=\xi-\Delta+\sqrt{\eta}\tanh(r)[\sqrt{\eta}\alpha-\sqrt{2}(x_a-ip_b)]$.

We can find the P-representation corresponding to the density operator $\hat{\rho}_b$ via the relation [19]

$$P_b(\gamma) = \frac{e^{|\gamma|^2}}{\pi^2}\int d^2\delta\left\langle -\delta\right|\hat{\rho}_b\left|\delta\right\rangle e^{|\delta|^2-\delta\gamma^*+\delta^*\gamma}. \tag{4.47}$$

It follows, on substituting for $\hat{\rho}_b$ from Eq. (15) into Eq. (16) and computing the integrals, that we have

$$\begin{aligned}P_b(\gamma) &= \frac{N}{\pi C}\int d^2\alpha P_i(\alpha)\\ &\quad \exp\{-\frac{D}{C}[\eta|\alpha|^2-\beta\sqrt{\eta}(\alpha\gamma^*+c.c.)+|\gamma|^*]\},\end{aligned} \tag{4.48}$$

where

$$C=\langle n\rangle(1-\beta^2)+(1+\langle n\rangle)[\beta-\sqrt{\eta}\tanh(r)]^2, \tag{4.49}$$

$$D=1-(1+\langle n\rangle)\eta\tanh^2(r). \tag{4.50}$$

In Eq. (17), we choose $\beta = 1/\sqrt{\eta}$ such that the fidelity of teleportation is maximal for a given squeezing parameter r and the teleported state is exactly same as the input state if r is infinite [70, 74], and the P-representation of the teleported field takes the form

$$P_b(\gamma) = \frac{1}{\pi s}\int d^2\alpha P_i(\alpha)\exp(-\frac{|\alpha-\gamma|^2}{s}), \tag{4.51}$$

where

$$s = e^{-2r} + \frac{1-\eta}{\eta}. \tag{4.52}$$

The relation (20) is the key result of this paper. We shall see that some important conclusions can be induced from this result.

For a given density matrix $\hat{\rho}$, there are different representations such as P-, Q- and Wigner-Weyl-representations, which are defined as [19]

$$P(\gamma) = tr[\rho\delta(\gamma^* - \hat{b}^\dagger)\delta(\gamma - \hat{b})], \tag{4.53}$$

$$Q(\gamma) = tr[\rho\delta(\gamma - \hat{b})\delta(\gamma^* - \hat{b}^\dagger)], \tag{4.54}$$

$$W(\gamma) = \frac{1}{\pi^2}\int d^2\beta e^{-i\beta\gamma^* - i\beta^*\gamma} tr[e^{i\beta\hat{b}^\dagger + i\beta^*\hat{b}}], \tag{4.55}$$

According to these definitions, we have the relations

$$Q(\gamma) = \frac{1}{\pi}\int d^2\beta e^{-|\beta-\gamma|^2} P(\beta), \tag{4.56}$$

$$W(\gamma) = \frac{2}{\pi}\int d^2\beta e^{-2|\beta-\gamma|^2} P(\beta). \tag{4.57}$$

It follows, on comparing Eqs. (25) and (26) with Eq. (20), we see that when s=1/2 or 1 the teleportation protocol changes the P-representation of the input state to the Wigner-Weyl-representation or Q-representation. For the case of the ideal detection, Caves and Wodkiewicz [76] showed that the Wigner function of the output state is

the Q-function of the input state when $s = 1/2$ or $e^{-2r} > 1/2$. We know that the Q-representation is always non-negative definite. However, the positivity of the Wigner function can not guarantee that the teleported states must be classical. Here,we showed that when s=1 the P-representation of the teleported field is certainly positive definite. Therefore, the teleported state must become classical no matter which kind and how highly nonclassical the input state is when $s > 1$ or

$$\eta \leq 1/(2 - e^{-2r}). \tag{4.58}$$

We also see that when $\eta < 0.5$ the teleported field is definitely classical even if the squeezing parameter approaches infinity. Ralph et al [77] obtained the same conclusion according to the condition that the variances of the phase-quadrature amplitudes of the output state is larger than 1/2. Here, we derive the conclusion based on the positivity of the P-function of the teleported state. We believe that our discussion makes the conclusion more reliable.

In the current experiment of continuous-variable teleportation [22], noise reduction in either the sum or subtraction of quadrature-phase amplitudes of the modes a and b can be more than 3 dB below vacuum noise. The corresponding squeezing parameter r is around 0.35. For this degree of suqeezing, from (27), we obtain the critical homodyne detection efficiency $\eta = 0.67$. Nonclassical properties of the input state may be preserved in the teleported state only when the homodyne detection efficiency $\eta > 0.67$. The efficiency of recent homodyne detection systems is around 90% [96]. Therefore, the preservation of nonclassicality may be realized in the current continuous-variable teleportation.

CHAPTER V

SUMMARY AND CONCLUSIONS

In conclusion, For entanglement generation we have shown three methods for preparing an arbitrary two-mode states. The first methods achieved by using atom-photon interaction inside cavities. The resulting states can be obtained with unit probability. We can extend this study to creating arbitrary two-mode N photons and multi-mode N photon states. The second method is to prepare an arbitrary two-mode atomic state in a system of two dipole-dipole interacting atoms. By applying a sequence of three suitable driving field pulses, any superposition of the four possible atomic states can be achieved. The last method is to prepare an arbitrary two-mode spin states via weak interaction between two spin system and radio frequency. The special energy levels in this system make two qubits entangled states generation problem be simplified to one qubit entangled state generation. We can also use off resonance radio frequency pulses to make desired states and this methods can be extend to other two-level quantum system such as two atom system where radio frequency will be replaced by driving field. We have also discussed a scheme for the implementation of quantum walk in a cavity QED system. This system allows us to study the properties of quantum walks in half space. For Quantum teleportation of an arbitrary superposition of atomic Dicke states, we anticipate that the main elements of the proposed scheme will be useful in a variety of quantum information applications beyond teleportation. A key feature of the scheme is the multi-atom adiabatic passage that enables mapping of atomic Dicke-state entanglement to the photonic degrees of freedom. This method should prove useful for large-scale transfer of entangled quantum information between matter systems, a key requirement for distributed quantum computing. Furthermore, it also suggests the possibility of entanglement transfer between unequal

number of atoms in both cavities, leading to applications such as dense coding and entanglement purification which can be fruitfully addressed with a mixed-state generalization of our scheme. And finally, we have reformulated the teleportation protocol for continuous variables of an optical field in the density matrix form explicitly including the effciency of the homodyne detections and established the relation between the P-functions of the input and teleported states. We show that in some cases the teleportation protocol transfers the P-representation of the input state to either the Wigner-Weyl-representation or Q-representation. The state-independent-condition under which the teleported field must be classical is found.

REFERENCES

[1] A. Einstein, B. Podolsky and N. Rosen, Phys. Rev. **47**, 777 (1935).

[2] C. H. Bennett, G. Brassard, C. Crepeau, R. Jozsa, A. Peres and W. K. Wootters, Phys. Rev. Lett. **70**, 1895 (1993).

[3] C. H. Bennett and S. J. Wiesner, Phys. Rev. Lett. **69**, 2881 (1992).

[4] A. K. Ekert, Phys. Rev. Lett. **67**, 6961 (1991).

[5] A. Barenco, D. Deutsch, A. Ekert and R. Jozsa, Phys. Rev. Lett. **74**, 4083 (1995).

[6] J. S. Bell, *Speakable and Unspeakable in Quantum Mechanics* (Cambridge Univ. Press, Cambridge, England, 1988), p. 196.

[7] K. Vogel, V. M. Akulin and W. P. Schleich, Phys. Rev. Lett. **71**, 1816 (1993).

[8] B. M. Garraway, B. Sherman, H. Moya-Cessa and P. L. Knight, Phys. Rev. A **49**, 535 (1994).

[9] C. K. Law and J. H. Eberly, Phys. Rev. Lett. **76**, 1055 (1996).

[10] A. S. Parkins, P. Marte, P. Zoller and H. J. Kimble, Phys. Rev. Lett. **71**, 3095 (1993); A. S. Parkins, P. Marte, P. Zoller, O. Carnal and H. J. Kimble, Phys. Rev. A **51**, 1578 (1995).

[11] C. K. Law and J. H. Eberly, J. Mod. Opt. **44**, 2149 (1997).

[12] D. M. Greenberger, M. Horne and A. Zeilinger, *in Bell's theorem*, edited by M. Kafatos(Kluwer, Dordrecht, 1989), p.69.

[13] M. S. Zubairy, Phys. Rev. A **58**, 4368 (1998).

[14] M. Ikram, S.-Y. Zhu and M. S. Zubairy, Opt. Commun. **184**, 417 (2000).

[15] S. Scheel and D. -G. Welsch, Phys. Rev. A **64**, 063811 (2001).

[16] L. -M. Duan and H. J. Kimble Phys. Rev. Lett. **90**, 253601 (2003).

[17] L. -M. Duan, A. Kuzmich and H. J. Kimble Phys. Rev. A **67**, 032305 (2003).

[18] T. Di and M. S. Zubairy, J. Mod. Optic **51** 2387 (2004).

[19] See, for example, M. O. Scully, M. S. Zubairy, *Quantum Optics* (Cambridge, London 1997).

[20] Z. Ficek and R. Tanas, Phys. Report **372**, 369 (2002).

[21] Z. Ficek and R. Tanas, Fortschr Phys.**51**, 230 (2003).

[22] G. M. Palma and P. L. Knight, Phys. Rev. A **39**,1962 (1989).

[23] Z. Ficek and P. D. Drummond, Phys. Today **50**,34 (1997).

[24] V. S. Malinovsky and I. R. Sola Phys. Rev. Lett. **93**, 190502 (2004).

[25] C. H. Bennett, G. Brassard, C. Crepeau, R. Jozsa, A. Peres and W. K. Wootters, Phys. Rev. Lett. **70**, 1895 (1993).

[26] C. P. Williams and S. H. Clearwater, *Exploration in Quantum Computing* (Springer, New York, 1998)

[27] R. G. Unanyan, B. W. Shore and K. Bergmann, Phys. Rev. A **63**, 043405 (2001).

[28] D. G. Cory, A. F. Fahmy and T. F. Havel, Proc. Natl. Acad Sci. U.S.A. **94**, 1634 (1997); N. A. Gershenfeld and I. L. Chuang, Science **275**, 350 (1997); J. A. Jones and M. Mosca, J. Chem. Phys. **109**, 1648 (1998).

[29] Y. Aharonov, L. Davidovich and N. Zagury, Phys. Rev. A **48** (2) 1687-1690 (1993).

[30] D. A. Meyer, Preprint quant-ph/9604011(1996).

[31] D. A. Meyer, Preprint quant-ph/9605023 (1996).

[32] D. A. Meyer, J. Stat. Phys. **85** (5-6): 551-574 (1996).

[33] J. Watrous, *in Proceedings of the 33rd Symposium on the Theory of Computing*(ACM Press, New York, 2001), p. 60.

[34] D. Aharanov, A. Ambainis, J. Kempe and U. Vazirani, *in Proceedings of the 33rd Symposium on the Theory of Computing*(ACM Press, New York, 2001), pp 50-59.

[35] A. Ambainis, E. Bach, A. Nayak, A. Vishwanath and J. Watrous, *in Proceedings of the 33rd Symposium on the Theory of Computing*(ACM Press, New York, 2001), pp 60-69. (2001).

[36] A. Nayak and A. Vishwanath, Preprint quant-ph/0010117 (2000).

[37] E. Farhi and S. Gutmann, Phys. Rev. A **58** 915 (1998).

[38] M. Hillery, J. Bergou and E. Feldman, Phys. Rev. A (in press).

[39] E. Bach, S. Coppersmith, M. P. Goldschen, R. Joynt and J. Watrous Quant-ph/0207008

[40] A. M. Childs, R. Cleve, E. Deotto, E. Farhi, S. Gutmann and D. A. Spielman, Preprint quant-ph/0209131 (2002).

[41] N. Shenvi, J. Kempe and K. B. Whaley, Phys. Rev. A **67** 052307 (2003)

[42] B. C. Travaglione and G. J. Milburn, quant-ph/0109076.

[43] W. Dür, R. Rausendorf, V. M. Kendon and H. -J. Briegel, quant-ph/0203037.

[44] B. C. Sanders, S. D. Bartlett, B. Treganna and P. L. Knight, quant-ph 0207028.

[45] Z. Zhao, J. Du, H. Li, T. Yang and J. -W. Pan, quant-ph/0212149.

[46] H. Jeong, M. Paternostro and M. S. Kim, quant-ph/0305003.

[47] P. L. Knight, E. Roldan and J. E. Sipe, quant-ph/0304201.

[48] P. L. Knight, E. Roldan and J. E. Sipe, quant-ph/0305165.

[49] D. Bouwmeester, I. Marzoli, G. P. Karman, W. Schleich and J. P. Woerdman, Phys. Rev. A **61**, 013410 (2000).

[50] D. Bouwmeester, J.-W. Pan, K. Mattle, M. Eibl, H. Weifurter and A. Zeilinger, Nature **390**, 575 (1997).

[51] A. Furusawa, J. L. Sorensen, S. L. Brounstein, C. A. Fuchs, H. J. Kimble, and E. S. Polzik, Science **282**, 706 (1998).

[52] L. Davidovich, N. Zagury, M. Brune, J.M. Raimond, and S. Haroche, Phys. Rev. A **50**, R895 (1994); J. I. Cirac and A. S. Parkins, Phys. Rev. A **50**, R4441 (1994); M. H. Y. Moussa, Phys. Rev. A **55**, R3287 (1997); S.-B. Zheng and G.-C. Guo, Phys. Lett. A **232**, 171 (1997).

[53] M. Riebe, H. Häffner, C. F. Roos, W. Hänsel, J. Benhelm, G. P. T. Lancaster, T. W. Körber, C. Becher, F. Schmidt-Kaler, D. F. V. James and R. Blatt, Nature **429**, 734 (2004); M. D. Barrett, J. Chiaverini, T. Schaetz, J. Britton, W. M. Itano, J. D. Jost, E. Knill, C. Langer, D. Leibfried, R. Ozeri and D. J. Wineland, Nature **429**, 737 (2004).

[54] M. Brune, S. Haroche, J. M. Raimond, L. Davidovich and N. Zagury, Phys. Rev. A **45**, 5193 (1992).

[55] L. Davidovich, A. Maali, M. Brune, J. M. Raimond and S. Haroche, Phys. Rev. Lett. **71**, 2360 (1993.)

[56] L. Davidovich, N. Zagury, M. Brune, J. M. Raimond and S. Haroche, Phys. Rev. A **50**, 895 (1994).

[57] J. J. Cirac and A. S. Parkins, Phys. Rev. A **50**, 4441 (1994).

[58] H. Weinfurt, Europhys. Lett. **25**, 559 (1994).

[59] M. H. Y. Moussa, Phys. Rev. A **55**, 3287 (1997).

[60] S. B. Zheng and G. C. Guo, Phys. Lett. A **232**, 171 (1997).

[61] L. Vaidman and N. Yoran, Phys. Rev. A **59**, 116 (1999).

[62] N. Linden and S. Popescu, Phys. Rev. A **59**, 137 (1999).

[63] A. Karlsson and M. Bourennane, Phys. Rev. A **58**, 4394 (1998).

[64] M. H. Y. Moussa, Phys. Rev. A **54**, 4661 (1996).

[65] S. Stenholm and P. J. Bardroff, Phys. Rev. A **58**, 4373 (1998).

[66] D. Bouwmeester, J. -W. Pan, K. Mattle, M. Eibl, H. Weinfurter and A. Zeilinger, Nature **390**, 575 (1997).

[67] D. Boschi1, S. Branca, F. De Martini1, L. Hardy, and S. Popescu, Phys. Rev. Lett. **80**, 1121 (1998).

[68] J. -W. Pan, S. Gasparoni, M. Aspelmeyer, T. Jennewein and A. Zeilinger, Nature **421**, 721 (2003).

[69] L. Vaidman, Phys. Rev. A **49**, 1473 (1994).

[70] S. L. Braunstein and H. J. Kimble, Phys. Rev. Lett. **80**, 869 (1998).

[71] A. Furusawa, J. L. Sϕrensen, S. L. Braunstein, C. A. Fuchs, H. J. Kimble and E. S. Polzik, Science **282**, 706 (1998).

[72] T.-C. Zhang, K. W. Goh, C. W. Chou, P. Lodahl and H. J. Kimble, Phys. Rev. A**67**, 033802 (2003).

[73] W. P. Bowen, N. Treps, B. C. Buchler, R. Schnabel, T. C. Ralph, H. -A. Bachor, T. Symul and P. K. Lam, Phys. Rev. A **67**, 032302 (2003).

[74] J. Y. Lee, M. S. Kim and H. S. Jeong, Phys. Rev. A **62**, 032305 (2000).

[75] F. L. Li, H. R. Li, J. X. Zhang and S. Y. Zhu, Phys. Rev. A **66**, 024302 (2002).

[76] C. M. Caves and K. Wodkiewicz, Phys. Rev. Lett. **93**, 040506 (2004).

[77] T. C. Ralph, P. K. Lam and R. E. S. Polkinghome, J. Opt. **B1**, 483 (1999).

[78] Z. Ficek and R. Tanas, S. Kielich, Physica A **146**, 452 (1987).

[79] Z. Ficek and R. Tanas, Phys. Report **372**, 369 (2002).

[80] S. Bose, P. L. Knight, M. B. Plenio and V. Vedral, Phys. Rev. Lett. **83**, 5158 (1999).

[81] C. Cabrillo, J. I. Cirac, P. Garca-Fernandez and P. Zoller, Phys. Rev. A **59**, 1025 (1999).

[82] M. B. Plenio, S. F. Huelga, A. Beige and P. L. Knight, Phys. Rev. A **59**, 2468 (1999); see also G. J. Yang, O. Zobay, and P. Meystre , Phys. Rev. A **59**, 4012 (1999).

[83] J. I. Cirac, P. Zoller, H. J. Kimble and H. Mabuchi, Phys. Rev. Lett. **78**, 3221 (1997); S. J. van Enk, H. J. Kimble, J. I. Cirac and P. Zoller, Phys. Rev. A **59**, 2659 (1999).

[84] T. Pellizzari, Phys. Rev. Lett. **79**, 5242 (1997).

[85] R. H. Dicke, Phys. Rev. **93**, 99 (1954).

[86] L. M. Duan and H. J. Kimble, Phys. Rev. Lett. **90**, 253601 (2003).

[87] M. B. Plenio and P. L. Knight, Rev. Mod. Phys. **70**, 101 (1998).

[88] J. Dalibard, Y. Castin and K. Molmer, Phys. Rev. Lett. **68**, 580 (1992).

[89] H. J. Carmichael, *An Open Systems Approach to Quantum Optics* (Springer-Verlag, Berlin, 1993).

[90] M. S. Shahriar, J. A. Bowers, B. Demsky, P. S. Bhatia, S. Lloyd, P. R. Hemmer and A. E. Craig, Optics Commun. **195**, 411 (2001).

[91] M. Sargent III, M. O. Scully and W. E. Lamb, Jr., *Laser Physics* (Addison-Wesley, Reading, MA, 1974), Appendix G.

[92] J. Ye, D. W. Vernooy and H. J. Kimble, Phys. Rev. Lett. **83**, 4987 (1999).

[93] D. Frese, B. Ueberholz, S. Kuhr, W. Alt, D. Schrader, V. Gomer, and D. Meschede, Phys. Rev. Lett. **85**, 3777 (2000).

[94] K. Banaszek and K. Wodkiewicz, Phys. Rev. A **55**, 3117(1997).

[95] U. Leonhardt and H. Paul, Phys. Rev. A **48**, 4598(1993).

[96] P. K. Lam , T. C. Ralph, B. C. Buchler D. E. McClelland, H-A Bachor and J Gao, J. Opt. B: Quantum Semicalss. Opt. **1**, 469(1999).

APPENDIX A

We give below the details of the calculation for the two-atom case below. After preparation, Alice waits until she hears two (and only two) clicks at $t = t_1$ and $t = t_2$, following which the state in cavity A is teleported to cavity B successfully. For simplicity, the normalization factors are suppressed in Eqs. (A.1)-(A.7) below.

From Eqs. (4.15) and (4.19), at the end of the preparation stage (defined as $t = 0$), we have

$$\begin{aligned}
|\Psi\rangle_{AB}^{\text{in}} &= |\Psi\rangle_A \otimes |\Psi\rangle_B \\
&= \Big[C_0 D_0 |bb\rangle_B |0\rangle_A |0\rangle_B + C_1 D_0 |bb\rangle_B |1\rangle_A |0\rangle_B \\
&\quad + C_2 D_0 |bb\rangle_B |2\rangle_A |0\rangle_B \\
&\quad + C_0 D_1 \frac{|bc\rangle_B + |cb\rangle_B}{\sqrt{2}} |0\rangle_A |1\rangle_B \\
&\quad + C_1 D_1 \frac{|bc\rangle_B + |cb\rangle_B}{\sqrt{2}} |1\rangle_A |1\rangle_B \\
&\quad + C_2 D_1 \frac{|bc\rangle_B + |cb\rangle_B}{\sqrt{2}} |2\rangle_A |1\rangle_B \\
&\quad + C_0 D_2 |cc\rangle_B |0\rangle_A |2\rangle_B + C_1 D_2 |cc\rangle_B |1\rangle_A |2\rangle_B \\
&\quad + C_2 D_2 |cc\rangle_B |2\rangle_A |2\rangle_B \Big] |cc\rangle_A .
\end{aligned} \tag{A.1}$$

When $t = t_1$, *before* Alice registers the first click, the joint state of Alice's and Bob's systems has evolved conditional on no detector click, according to the evolution

operator $\exp(-\kappa\hat{a}^{\dagger}\hat{a}t_1)$ for photons in each cavity:

$$
\begin{aligned}
|\Psi(t_1)\rangle \;=\; & \Big[C_0D_0|bb\rangle_B|0\rangle_A|0\rangle_B \\
& +C_1D_0e^{-\kappa t_1}|bb\rangle_B|1\rangle_A|0\rangle_B \\
& +C_2D_0e^{-2\kappa t_1}|bb\rangle_B|2\rangle_A|0\rangle_B \\
& +C_0D_1e^{-\kappa t_1}\frac{|bc\rangle_B+|cb\rangle_B}{\sqrt{2}}|0\rangle_A|1\rangle_B \\
& +C_1D_1e^{-2\kappa t_1}\frac{|bc\rangle_B+|cb\rangle_B}{\sqrt{2}}|1\rangle_A|1\rangle_B \\
& +C_2D_1e^{-3\kappa t_1}\frac{|bc\rangle_B+|cb\rangle_B}{\sqrt{2}}|2\rangle_A|1\rangle_B \\
& +C_0D_2e^{-2\kappa t_1}|cc\rangle_B|0\rangle_A|2\rangle_B \\
& +C_1D_2e^{-3\kappa t_1}|cc\rangle_B|1\rangle_A|2\rangle_B \\
& +C_2D_2e^{-4\kappa t_1}|cc\rangle_B|2\rangle_A|2\rangle_B\Big]|cc\rangle_A. \qquad \text{(A.2)}
\end{aligned}
$$

Then the first click occurs and the time evolution of the system state is interrupted by a quantum jump at one of the two detectors D_+ or D_-. For the D_+ detector, we

find

$$
\begin{aligned}
\hat{D}_+|\Psi(t_1)\rangle &= (ta_A + ra_B)|\Psi(t_1)\rangle \\
&= [C_1 D_0 t e^{-\kappa t_1}|bb\rangle_B|0\rangle_A|0\rangle_B \\
&\quad +\sqrt{2}C_2 D_0 t e^{-2\kappa t_1}|bb\rangle_B|1\rangle_A|0\rangle_B \\
&\quad +C_0 D_1 r e^{-\kappa t_1}\frac{|bc\rangle_B + |cb\rangle_B}{\sqrt{2}}|0\rangle_A|0\rangle_B \\
&\quad +C_1 D_1 t e^{-2\kappa t_1}\frac{|bc\rangle_B + |cb\rangle_B}{\sqrt{2}}|0\rangle_A|1\rangle_B \\
&\quad +C_1 D_1 r e^{-2\kappa t_1}\frac{|bc\rangle_B + |cb\rangle_B}{\sqrt{2}}|1\rangle_A|0\rangle_B \\
&\quad +\sqrt{2}C_2 D_1 t e^{-3\kappa t_1}\frac{|bc\rangle_B + |cb\rangle_B}{\sqrt{2}}|1\rangle_A|1\rangle_B \\
&\quad +C_2 D_1 r e^{-3\kappa t_1}\frac{|bc\rangle_B + |cb\rangle_B}{\sqrt{2}}|2\rangle_A|0\rangle_B \\
&\quad +\sqrt{2}C_0 D_2 r e^{-2\kappa t_1}|cc\rangle_B|0\rangle_A|1\rangle_B \\
&\quad +C_1 D_2 t e^{-3\kappa t_1}|cc\rangle_B|0\rangle_A|2\rangle_B \\
&\quad +\sqrt{2}C_1 D_2 r e^{-3\kappa t_1}|cc\rangle_B|1\rangle_A|1\rangle_B \\
&\quad +\sqrt{2}C_2 D_2 t e^{-4\kappa t_1}|cc\rangle_B|1\rangle_A|2\rangle_B \\
&\quad +\sqrt{2}C_2 D_2 r e^{-4\kappa t_1}|cc\rangle_B|2\rangle_A|1\rangle_B]|cc\rangle_A, \\
&\equiv |\Psi_+(t_1)\rangle, \qquad \text{(A.3)}
\end{aligned}
$$

while for D_- we have an analogous result with $t \to r$ and $r \to -t$. During the period $t_2 - t_1$, no clicks occur again by definition and the above state evolves according to

$\exp[-\kappa\hat{a}^\dagger\hat{a}(t_2-t_1)]$:

$$
\begin{aligned}
|\Psi_+(t_2)\rangle \;=\; & e^{-\kappa t_1}[C_1D_0t|bb\rangle_B|0\rangle_A|0\rangle_B \\
& +\sqrt{2}C_2D_0te^{-\kappa t_2}|bb\rangle_B|1\rangle_A|0\rangle_B \\
& +C_0D_1r\frac{|bc\rangle_B+|cb\rangle_B}{\sqrt{2}}|0\rangle_A|0\rangle_B \\
& +C_1D_1te^{-\kappa t_2}\frac{|bc\rangle_B+|cb\rangle_B}{\sqrt{2}}|0\rangle_A|1\rangle_B \\
& +C_1D_1re^{-\kappa t_2}\frac{|bc\rangle_B+|cb\rangle_B}{\sqrt{2}}|1\rangle_A|0\rangle_B \\
& +\sqrt{2}C_2D_1te^{-2\kappa t_2}\frac{|bc\rangle_B+|cb\rangle_B}{\sqrt{2}}|1\rangle_A|1\rangle_B \\
& +C_2D_1re^{-2\kappa t_2}\frac{|bc\rangle_B+|cb\rangle_B}{\sqrt{2}}|2\rangle_A|0\rangle_B \\
& +\sqrt{2}C_0D_2re^{-\kappa t_2}|cc\rangle_B|0\rangle_A|1\rangle_B \\
& +C_1D_2te^{-2\kappa t_2}|cc\rangle_B|0\rangle_A|2\rangle_B \\
& +\sqrt{2}C_1D_2re^{-2\kappa t_2}|cc\rangle_B|1\rangle_A|1\rangle_B \\
& +\sqrt{2}C_2D_2te^{-3\kappa t_2}|cc\rangle_B|1\rangle_A|2\rangle_B \\
& +\sqrt{2}C_2D_2re^{-3\kappa t_2}|cc\rangle_B|2\rangle_A|1\rangle_B]|cc\rangle_A,
\end{aligned}
\tag{A.4}
$$

with an analogous result for $|\Psi_-(t_2)\rangle$ with $t \to r$ and $r \to -t$. Now the second click occurs at $t = t_2$. For the detection scenario D_+D_+, we find that the final state is:

$$\begin{aligned}
\hat{D}_+|\Psi_+(t_2)\rangle &= (ta_A + ra_B)|\Psi_+(t_2)\rangle \\
&= \sqrt{2}e^{-\kappa t_1 - \kappa t_2}[(C_0 D_2 r^2 |cc\rangle_B \\
&\quad + \sqrt{2}C_1 D_1 tr \frac{|bc\rangle_B + |cb\rangle_B}{\sqrt{2}} \\
&\quad + C_2 D_0 t^2 |bb\rangle_B)|0\rangle_A|0\rangle_B \\
&\quad + e^{-\kappa t_2}(C_1 D_2 (2tr|cc\rangle_B|0\rangle_A|1\rangle_B \\
&\quad + r^2|cc\rangle_B|1\rangle_A|0\rangle_B) \\
&\quad + C_2 D_1 (t^2|cc\rangle_B|0\rangle_A|1\rangle_B \\
&\quad + 2tr|cc\rangle_B|1\rangle_A|0\rangle_B)) \\
&\quad + e^{-2\kappa t_2} C_2 D_2 (t^2|cc\rangle_B|0\rangle_A|2\rangle_B \\
&\quad + 2\sqrt{2}rt|cc\rangle_B|1\rangle_A|1\rangle_B \\
&\quad + r^2|cc\rangle_B|2\rangle_A|0\rangle_B)].
\end{aligned} \tag{A.5}$$

For the detection scenario D_-D_+ or D_+D_-, we find:

$$\begin{aligned}
\hat{D}_-|\Psi_+(t_2)\rangle &= (ra_A - ta_B)|\Psi_+(t_2)\rangle \\
&= \sqrt{2}e^{-\kappa t_1-\kappa t_2}[(-\sqrt{2}C_0D_2rt|cc\rangle_B \\
&\quad +(-t^2+r^2)C_1D_1\frac{|bc\rangle_B+|cb\rangle_B}{\sqrt{2}} \\
&\quad +C_2D_0\sqrt{2}tr|bb\rangle_B)|0\rangle_A|0\rangle_B \\
&\quad +e^{-\kappa t_2}(C_1D_2((-t^2+r^2)|cc\rangle_B|0\rangle_A|1\rangle_B \\
&\quad -rt|cc\rangle_B|1\rangle_A|0\rangle_B) \\
&\quad +C_2D_1(rt|cc\rangle_B|0\rangle_A|1\rangle_B \\
&\quad +(-t^2+r^2)|cc\rangle_B|1\rangle_A|0\rangle_B)) \\
&\quad +e^{-2\kappa t_2}C_2D_2(t^2|cc\rangle_B|0\rangle_A|2\rangle_B \\
&\quad +2\sqrt{2}rt|cc\rangle_B|1\rangle_A|1\rangle_B \\
&\quad +r^2|cc\rangle_B|2\rangle_A|0\rangle_B)].
\end{aligned} \tag{A.6}$$

Finally for the detection scenario D_-D_-, we find:

$$\begin{aligned}
\hat{D}_-|\Psi_-(t_2)\rangle &= (ra_A - ta_B)|\Psi_-(t_2)\rangle \\
&= \sqrt{2}e^{-\kappa t_1-\kappa t_2}[(C_0D_2t^2|cc\rangle_B \\
&\quad -\sqrt{2}C_1D_1tr\frac{|bc\rangle_B + |cb\rangle_B}{\sqrt{2}} \\
&\quad +C_2D_0r^2|bb\rangle_B)|0\rangle_A|0\rangle_B \\
&\quad +e^{-\kappa t_2}(C_1D_2(-2rt|cc\rangle_B|0\rangle_A|1\rangle_B \\
&\quad +t^2|cc\rangle_B|1\rangle_A|0\rangle_B) \\
&\quad +C_2D_1(r^2|cc\rangle_B|0\rangle_A|1\rangle_B \\
&\quad -2tr|cc\rangle_B|1\rangle_A|0\rangle_B)) \\
&\quad +e^{-2\kappa t_2}C_2D_2(r^2|cc\rangle_B|0\rangle_A|2\rangle_B \\
&\quad -2\sqrt{2}rt|cc\rangle_B|1\rangle_A|1\rangle_B \\
&\quad +t^2|cc\rangle_B|2\rangle_A|0\rangle_B)].
\end{aligned} \tag{A.7}$$

In all cases, we can write the final atom-field state (upon two detection events) as in Eqs. (4.24) and (4.25), where the pre-factors η_m given in Figure 14 may be read out from the $|0\rangle_A|0\rangle_B$ component of Eqs. (A.5-A.7), making the substitutions for C_p and D_p in Eqs. (4.16-4.18) and (4.20-4.22).

VITA

Name: Tiegang Di

Address:

Department of Physics

Texas A&M University

College Station

TX 77843-4242

EDUCATION

Texas A&M University, College Station, TX

Ph.D. in Physics, Theoretical Optics, **May 2006**

M.S. in Physics, Theoretical Physics, **May 2002**

JiLin University, Chang Chun, JiLin, P. R. China

B.S. in Physics, Theoretical Physics, **May 1992**

M.S. in Physics, Theoretical Physics, **May 1995**

The typist for this dissertation was Tiegang Di.